

Topical Report

AMBIENT AND HIGH-TEMPERATURE CALORIMETRY OF COMMERCIAL SURFACTANTS

Project BE4A, Milestone 8, FY89 Annual Research Plan

by Leo A. Noll

**Work Performed for the
Department of Energy
Under Cooperative Agreement
DE-FC22-83FE60149**

**Jerry Casteel, Project Manager
Bartlesville Project Office
Department of Energy**

DISCLAIMER

This report was prepared as an account of work sponsored by an agency of the United States Government. Neither the United States Government nor any agency thereof, nor any of their employees, makes any warranty, express or implied, or assumes any legal liability or responsibility for the accuracy, completeness, or usefulness of any information, apparatus, product, or process disclosed, or represents that its use would not infringe privately owned rights. Reference herein to any specific commercial product, process, or service by trade name, trademark, manufacturer, or otherwise, does not necessarily constitute or imply its endorsement, recommendation, or favoring by the United States Government or any agency thereof. The views and opinions of authors expressed herein do not necessarily state or reflect those of the United States Government or any agency thereof.

**IIT Research Institute
National Institute for Petroleum and Energy Research
P.O. Box 2128
Bartlesville, Oklahoma 74005**

TABLE OF CONTENTS

	<u>Page</u>
Abstract	1
Introduction.....	1
Acknowledgments.....	3
Experimental.....	3
Results and Discussion.....	4
Conclusions.....	8
References.....	9

TABLES

1. Properties of bulk surfactants	10
2. Density of Chevron Chaser SD1000 at 25° C	10
3. Density of Shamrock Sellogen WL at 25° C	11
4. Density of Shell Enordet AOS 1416 at 25° C.....	11
5. Density of Hüls CES 6.5 at 25° C	12
6. Density of Sandopan MA-18 at 25° C.....	12
7. Density of equimolar mixture of Enordet AOS 1416 and MA-18 at 25° C	13
8. Surface tensions at 25° C	13
9. Enthalpies of dilution of Chaser SD1000 at 25° C	14
10. Enthalpies of dilution of Chaser SD1000 at 125° C.....	15
11. Enthalpies of dilution of Chaser SD1000 at 200° C	16
12. Enthalpies of dilution of Sellogen WL at 25° C.....	17
13. Enthalpies of dilution of Sellogen WL at 125° C.....	18
14. Enthalpies of dilution of Sellogen WL at 200° C.....	19
15. Enthalpies of dilution of Enordet AOS 1416 at 25° C	20
16. Enthalpies of dilution of Enordet AOS 1416 at 125° C.....	21
17. Enthalpies of dilution of Enordet AOS 1416 at 200° C	22
18. Enthalpies of dilution of Hüls' CES 6.5 at 25° C	23
19. Enthalpies of dilution of Hüls' CES 6.5 at 125° C	24
20. Enthalpies of dilution of MA-18 at 25° C	25
21. Enthalpies of dilution of MA-18 at 125° C	26
22. Enthalpies of dilution of AOS / Ma-18 mixture at 25° C	27
23. Enthalpies of dilution of AOS / MA-18 mixture at 125 °C.....	29
24. Knot positions from the isothermal fits of Chaser SD1000.....	30

TABLES -- continued

	<u>Page</u>
25. Knot positions from the isothermal fits of Sellogen WL	31
26. Knot positions from the isothermal fits of Enordet AOS 1416.....	32
27. Knot positions from the isothermal fits of Hüls' CES 6.5.....	33
28. Knot positions from the isothermal fits of Sandopan MA-18.....	33
29. Knot positions from the isothermal fits of AOS / MA-18 mixture	34
30. Results of cubic spline fit L_ϕ data for Chaser SD1000	35
31. Results of cubic spline fit L_ϕ data for Sellogen WL.....	38
32. Results of cubic spline fit L_ϕ data for Enordet AOS 1416	40
33. Results of cubic spline fit L_ϕ data for Hüls' 6.5 CES.....	42
34. Results of cubic spline fit L_ϕ data for MA-18	44
35. Results of cubic spline fit L_ϕ data for AOS / Ma-18 mixture.....	46
36. CMC's of surfactants in percent active	47

ILLUSTRATIONS

1. Density of aqueous Chevron's Chaser SD1000 at 25° C.....	48
2. Surface tension of Chaser SD1000 as a function of log concentration at 25° C.....	48
3. Surface tension of Sellogen WL as a function of log concentration at 25° C.....	49
4. Surface tension of Enordet AOS 1416 as a function of log concentration at 25° C.....	49
5. Comparison of surface tension and relative apparent molar enthalpies of Sellogen WL at 25° C.....	50
6. Features of a relative apparent molar enthalpy plot	50
7. Relative apparent molar enthalpies of Chaser SD1000 at 25°, 125°, and 200° C.....	51
8. Relative apparent molar enthalpies of Sellogen WL at 25°, 125°, and 200° C	51
9. Relative apparent molar enthalpies of Enordet AOS 1416 at 25°, 125°, and 200° C.....	52
10. Relative apparent molar enthalpies of Hüls' 6.5 CES at 25° and 125° C.....	52
11. Relative apparent molar enthalpies of Sandopan MA-18 at 25° and 125° C.....	53
12. Relative apparent molar enthalpies of AOS / MA-18 mixture at 25° and 125° C.....	53

**AMBIENT AND HIGH-TEMPERATURE CALORIMETRY OF COMMERCIAL
SURFACTANTS**

By Leo A. Noll

ABSTRACT

Knowledge of the critical micelle concentration (CMC) is required for the effective use of surfactants for steamflooding, surfactant enhanced oil recovery, and process applications. The CMC's and solution behavior of commercial surfactants as a function of temperature were studied by dilution calorimetry.

The surfactants selected were Chevron's Chaser SD1000, a good foamer; Shell's Enordet AOS 1416, an intermediate foamer; and Diamond-Shamrock's Sellogen WL, a poor foamer. Although Sellogen is not intended to be used as a steam additive, it was included to emphasize differences between good and poor foamers. In addition to these surfactants, two carboxymethylated ethoxylated surfactants were used: Hüls' B498 and Sandoz's Sandopan MA-18. These surfactants were included because they have very different molecular structures from the first three, and because they have been proposed for use in high-temperature chemical floods. Finally, a mixture of Enordet and MA-18 was tested as an example of mixed surfactant types.

Of the steamflood additives tested, the Chaser has the lowest CMC at all temperatures. The height of the endothermal peak at 125° and 200° C is Enordet > Sellogen > Chaser. The broadness of the CMC region is Sellogen >> Enordet > Chaser at all temperatures. In general, the plateau is ordered Chaser < Enordet < Sellogen.

Effectiveness as a foamer is associated with a narrower CMC region and a more exothermic plateau region. This suggests that Chaser is able to form aggregates at 200° C in electrolyte-free water, while the others are not.

Ethoxylated carboxylates have solution properties distinctly different from those of sulfonate surfactants. A mixture of Enordet and MA-18 behaves like more dilute Enordet at 25° C, but much like the MA-18 at 125° C. This result suggests that if one wishes to incorporate some of the properties of an ethoxylated surfactant to an alpha olefin sulfonate (AOS) by mixing, an equimolar mixture may well be appropriate at 25° C, but at 125°, the molar ratio of CES must be much lower than 1:1.

INTRODUCTION

Surfactants at high temperatures are used for enhanced oil recovery (EOR) from high-temperature reservoirs as part of chemical slugs, and as additives in steamflooding to generate foams for the

emulsifiers for polymerization and other reactions, and as inhibitors in boiler and steam-handling equipment. In all of these applications, knowledge of the CMC as well as the ability to calculate activity coefficients at various temperatures (e.g. for solubility, CMC, and phase behavior properties) is vital to their successful, or at least more economic, implementation.

Petroleum sulfonates have historically been used as commercial surfactants for EOR. These surfactants are relatively low in cost and have good oil recovery properties, but in general do not perform well in the presence of high-salinity brines. Traditionally, cosurfactants or cosolvents consisting of short-chain alcohols have been used to increase salinity tolerance of surfactants. Unfortunately, mixtures of surfactants and alcohols are subject to preferential partitioning into the oil phase and to chromatographic separation of slug components while moving through the reservoir, which can cause loss of effectiveness of the chemical slug. Nonionic surfactants have better salt tolerance than ionic surfactants, but suffer from greater adsorption onto reservoir rocks and a tendency to form separate phases at temperatures above the cloud point. Mixtures of nonionic and anionic surfactants have been used to impart some of the nonionic qualities to the ionic materials. Chromatographic separation can affect these mixtures, and sometimes such a mixture will form a coacervate (a phase that can be very viscous).

Carboxymethylated ethoxylated (CES) materials of Hüls and Sandoz are commercial surfactants designed for high-temperature surfactant flooding, whereas Chevron has developed mixed alkyl sulfonates, and Shell has a line of alpha olefin sulfonates for steam additives. In addition to these materials, this report considers solution properties of a mixture of a sulfonate and a CES. The CES material was used for two reasons: firstly, some adsorption work is being performed at NIPER involving mixtures of CES and an anionic surfactant; secondly, since the CES does not phase separate at 100° C (as do many nonionic surfactants) nor does it form a coacervate, it is a way to approximate a mixture of anionic with nonionic surfactants whose properties may be examined at 125° C (257° F).

A series of NIPER technical papers¹⁻⁷ has described effects of temperature, chain length, alcohol, and electrolyte concentration on CMCs, relative apparent partial molar enthalpies, and heat capacities of aqueous surfactant solutions.

This report describes the effects of temperature on CMC's of commercial surfactants used as additives for steamflooding and high-temperature chemical floods. For greatest effectiveness, surfactants must be used at concentrations above the CMC. Thus, an investigation of the behavior of the CMC of surfactants as a function of temperature is highly important to their application. One of the purposes of this study was to compare solution properties of a good foamer (Chaser SD1000), an intermediate foamer (Enordet AOS 1416), and a poor foamer (Sellogen WL).

Three of the surfactants investigated in this project are sulfonates. Of these three sulfonate surfactants, Chevron's Chaser SD1000 and Shell's Enordet AOS 1416 have been applied in steam flooding. The third surfactant, Diamond Shamrock's Sellogen WL, was not intended by the manufacturer as a high-temperature product. It has been included for comparison purposes: to emphasize the differences in behavior of the sulfonates. In addition to the sulfonates, two surfactants of different structure were investigated -- carboxymethylated ethoxylated surfactants. These materials are composed of sodium carboxylate head groups, a series of ethylene oxide (EO) groups, and a hydrophobe. Hüls' B498 (CES 6.5) is an i-nonylphenol moiety with an average of 6.5 EO's, and Sandoz' Sandopan MA-18 is a n-nonylphenol with an average of 9 EO's. These materials have higher salinity tolerances than most sulfonate surfactants, and their dilution behaviors are considerably different from those of sulfonate materials.

ACKNOWLEDGMENTS

This work was sponsored by the U.S. Department of Energy under cooperative agreement DE-FC22-83FE60149.

EXPERIMENTAL

The effect of temperature on the micellization of commercial surfactants has been studied by the use of solution calorimetry. The technique used in this investigation is enthalpy of dilution measurements of aqueous surfactant solutions. High-temperature experiments were carried out by means of the Albert-Wood mass flow, temperature-rise calorimeter, and ambient experiments were run in an LKB System 2107 dilution calorimeter. References 1 through 7 describe the use of the high-temperature calorimeter, and reference 8 describes the LKB calorimeter. The precision of replicate measurements of large enthalpies is generally better than $\pm 1\%$.

The first three surfactants chosen were Chevron Chaser SD1000, a good foamer; Diamond Shamrock Sellogen WL, a poor foamer; and Shell Enordet AOS 1416, whose foaming behavior is intermediate between the other two. In addition to these surfactants, two carboxyethoxylated surfactants of interest for high-temperature chemical floods were selected: Hüls B498 (i-nonylphenol hydrophobe with 6.5 EO's) and Sandoz's Sandopan MA-18 (n-nonylphenol with 9 EO's). The latter surfactants have good temperature and salt tolerance. They also are very similar to nonionic surfactants, but have a high enough cloud point to permit dilution experiments at 125° C. In addition to these surfactants, the dilution behavior of a 1:1 molar mixture of Enordet and MA-18 was investigated. The percent active material, average molecular weight, and inorganic content of these surfactants are shown in table 1.

All surfactants were dissolved in and diluted with distilled deionized water. The MA-18 surfactant was obtained in acid form; thus it was necessary to neutralize the solutions with aqueous NaOH before dilution calorimetry measurements. Dilution experiments were carried out at 25° and 125° C for all surfactants and at 200° C for Chaser, Sellogen, and Enordet surfactants. Dilution ratios of surfactant solution to water were 3:2, 1:1, and 2:3. Ten solutions were made for each surfactant at nominal (bulk) concentrations of 0.25 to 20% by weight using distilled water as the solvent.

For ambient temperature dilution experiments, the mass flow rate of liquids was determined by weighing the bottles and measuring the time of flow. These flow rates were measured to better than $\pm 0.1\%$. For high-temperature experiments, the volumetric flow rates of the solvent and of the sample stream were measured to a precision of better than $\pm 0.3\%$. To calculate mass flow rates of reagents, the densities of their solutions are required. These densities were measured at 25° C and 1 atm with a Sodev vibrating tube densimeter, which is accurate to a few parts per million. Densities at higher pressures were calculated by assuming that compressibilities of the solutions were equal to that of pure water. Since the concentrations of solutes in solution were relatively small (<0.7 m), this was a reasonable approximation.

Surface tension measurements of aqueous surfactant solutions were made at 25° C with a Du Nouy ring tensiometer.

RESULTS AND DISCUSSION

The density of each aqueous surfactant solution is required for heat of dilution calculations. These densities along with linear least-squares fits to the density data are presented in tables 2 through 7. The plot of density vs. mass percent active surfactant for Chaser SD1000 is shown in figure 1, the line being the least-squares linear fit to the points. The plots of the other surfactants are similar, so they have not been shown. Tables 2 through 7 also include the apparent molar volumes, V_ϕ , which were calculated from⁹

$$V_\phi = M/d - [1000(d-d^\circ)/mdd^\circ] \quad (1)$$

where M is the molecular weight of solute, d is the density of solution, m is the molality of solution, and d° is the density of solvent.

Apparent molar volumes for all surfactants are only slightly dependent on concentration, increasing but slowly as concentration increases. The V_ϕ for the equimolar mixture of Enordet AOS and MA-18 is just about half way between the V_ϕ 's of the components. The normal behavior of V_ϕ vs. concentration for

pure surfactants is to remain at a low, relatively constant quantity up to the CMC, where it increases to an upper, relatively constant plateau value. The only surfactant having a CMC low enough to be within the range of density vs. concentration values is Sellogen WL, and it does not show this behavior; in general it slowly increases with concentration. This seems to be because it is a mixture of surfactant molecules, not an isomerically pure material, and therefore the break in the density line is not distinctly noticeable.

To relate the enthalpy of dilution measurements to the CMC of surfactants, surface tensions of aqueous solutions of Chaser SD1000, Sellogen WL, and Enordet 1416 were measured at 25° C. Surface tension results are given in table 8 and plotted in figures 2 through 4. In these figures, the solid lines simply connect the experimental points as an aid to the eye. The CMC of each surfactant is shown by the intersection of the dotted lines, which are the extrapolation of the surface tension of high- and low-concentration regions. In figures 3 and 4, the plots for Sellogen WL and Enordet AOS 1416, a dip occurs in the surface tension plot. This is an indication that they are mixed surfactants; that is, not isomerically pure. The CMC of Chaser SD1000 occurs at such a low concentration that the dip is not easily seen in the scatter of the data. CMC's from the surface-tension measurements are tabulated together with those derived from the enthalpy of dilution experiments in table 36. The CMC of Chaser is an order of magnitude lower than that of Enordet, which is an order of magnitude lower than Sellogen, even though they all have about the same average molar mass. A comparison of the surface-tension results with the relative apparent molar enthalpy results for Sellogen WL is shown in figure 5. For dilution calorimetry experiments, the CMC is assigned to the break in the L_ϕ curve (see below). The agreement of the determination of the CMC by both techniques is good -- 0.32% for the surface tension method and 0.44% for the heat of dilution method.

Enthalpies of dilution of all surfactants were measured at 25° and 125° C, whereas those of Chaser, Sellogen, and Enordet were measured at 200° C. The experimentally measured values of $\Delta_{\text{dil}}H$ are given in tables 9 through 23. In these tables, P is the backpressure used to ensure that the contents of the calorimeter remained as a single liquid phase; σ is the standard deviation of a point in the cubic spline fit; columns 1 and 2 list the initial and final surfactant molalities for each dilution, and column 3 gives the experimentally observed enthalpy change for that dilution. Column 4 lists the residual, which is the experimental enthalpy minus the fitted enthalpy, and column 5 gives the reciprocal of the weight of the point.

The enthalpies of dilution are the chords of a plot of relative apparent molal enthalpy (L_ϕ) as a function of surfactant molality concentration. The L_ϕ curve is developed by fitting the experimental data by a cubic spline technique,¹ which maintains continuous first and second derivatives. The routine generates a series of cubic polynomials joining a set of points referred to as "knots." The value of the first derivative of L_ϕ vs. concentration at low concentration is determined by the Debye-Hückel limiting law for a

1:1 electrolyte, such as NaCl; the value of L_ϕ at zero concentration is constrained to be zero. The knots used for the cubic spline fit are shown in tables 24 through 29. The least-squares fits to the experimental values are given in tables 30 through 35 and displayed in figures 7 through 12.

Figure 6 shows several features of the plots of relative apparent molal enthalpy (L_ϕ), (figs. 7 through 12). Figure 6 is the cubic spline fit for Enordet AOS 1416 at 125° C. In figure 6, region 1 is the premicellar or preaggregate region. In this example, this region shows positive nonideality, possibly caused by impurities, ion paring, and premicellar aggregation. For pure surfactants, this region has much lower enthalpies: 1 to 2 kJ/mol for the alkyltrimethylammonium bromides.¹⁻⁴ Lower enthalpy is also the case for 25° experiments for all surfactants measured.

Region 2 is the micellar region. The center of this region ("break in the curve") is considered as the CMC, although the CMC is a range of concentrations. The onset of micellization occurred throughout this region. In general, this region moves to a higher concentration and becomes broader and more diffuse as temperature increases.

In region 3, the enthalpy is sharply dependent on concentration. As concentration increases in this region, the fraction of the surfactant in micelles increases, and the curve reflects this exothermic heat of micellization. In region 4, the activity of micelles or aggregates has become a relatively constant and so has the fraction of surfactant in micellar form.

Figure 7 shows the results for Chaser SD1000. In this figure, note that the curve for 25° does not show a break in the experimentally accessible region; the CMC is 0.0032% by surface-tension measurements. The data at 125° C show a clear break in the curve at 0.11%, and the data for 200° show a break at 0.23%. (See table 36 for a complete listing of CMC's.) Thus, as temperature increases, the CMC moves to higher concentrations, and region 2 becomes broader. There is a correlation between the broadness of region 2, and the lowering of the cooperativity of micellization. The position of the break in the curves in figure 7 indicates that as the temperature increases, the CMC increases; change of the shape of the curves with temperature suggests that increasing temperature decreases the cooperativity of micellization, which is believed to be caused in part by a decrease in the micelle aggregation number.

The same general trends are noted for Sellogen WL (fig. 8) and Enordet AOS 1416 (fig. 9). The differences between Enordet and Chaser are that the Enordet has a higher CMC at all temperatures than does the Chaser. For Sellogen, the CMC is high enough that it appears in the 25° C curve; at 125° C the CMC is high and the curve quite diffuse; whereas at 200° no CMC region appears.

In comparing figures 7, 8, and 9, the following observations may be made:

1. The L_ϕ values for Chaser at high concentrations eventually become negative at each temperature.
2. For Enordet, the L_ϕ values become negative only for 25° C.
3. For Sellogen, the L_ϕ values never really become negative.
4. Sellogen is the only surfactant which appears to have an endothermal heat of micellization at 25° C.
5. For Sellogen at 200° C, the L_ϕ curve never trends toward lower endothermic values.
6. The height of the endothermal peak at 125° and 200° C is Enordet > Sellogen > Chaser.
7. The broadness of the CMC region (region 2) is Sellogen >> Enordet > Chaser at all temperatures.
8. Plateau values of L_ϕ are Chaser < Enordet < Sellogen.
9. Effectiveness as a foamer is associated with a narrower CMC (region 2) and a more exothermic plateau region. This suggests that Chaser is able to form aggregates at 200° C in electrolyte-free water, whereas the others are not.
10. A comparison with results for a pure surfactant DDTAB^{3,6-7} shows that for DDTAB the plateau of the L_ϕ curve reaches negative values at all temperatures up to 175° C, it becomes more endothermic as the temperature increases, and the broadness of the CMC region increases with increasing temperature. Also with increasing brine salinity, at a fixed temperature, the CMC decreases, the broadness of the CMC decreases, and the plateau region becomes more exothermic.

The curves for the carboxylated ethoxylated surfactants (figure 10 for Hüls 6.5 and figure 11 for MA-18) are quite different than those of the sulfonates, but quite similar to each other. The reason for this similarity is that the i-C₉ group in the Hüls surfactant is less hydrophobic than the n-C₉ group of the MA-18, but the MA-18 has 9 EO's as contrasted with 6.5 EO's for the Hüls. The large endothermic peaks seen in the high-temperature plots of Chaser, Sellogen, and Enordet no longer appear. This is partly because all dilution data for the CES surfactants have been taken above the CMC, and partly because the molecular structure is different and may be partly due to the fact that dilution experiments cannot be performed below the CMC.

For the mixed surfactant (fig. 12), the low-temperature curve is a bit closer to the behavior of Enordet than to the average, suggesting that some of the MA-18 is being incorporated into mixed

micelles by the Enordet. The high-temperature curve has almost identical behavior to that of MA-18 at that temperature. The mixture has a CMC much lower than that of the Enordet. The plateau value for the L_ϕ curve, which is identical with the MA-18, suggests that the MA-18 has strong enough interactions to prevent the aggregation of the Enordet or the Enordet is being incorporated into mixed micelles with the MA-18 in such a way as to impart the properties of the MA-18 aggregates. This result suggests that to incorporate some of the properties of an ethoxylated surfactant to an AOS by mixing the two types, an equimolar mixture may well be appropriate at 25° C, but at 125° C, the molar ratio of CES needs to be lower than 1:1.

CONCLUSIONS

1. Of the sulfonate type surfactants, Chaser SD1000 has the lowest CMC at all three temperatures.
2. At 200° C in the absence of brine, Chaser SD1000 needs to be present at 0.23% to be above the CMC, whereas Enordet AOS 1416 needs to be present at a 1.3% level.
3. The height of the endothermal peak at 125° and 200° C is Enordet > Sellogen > Chaser.
4. The broadness of the CMC region (region 2) is Sellogen >> Enordet > Chaser at all temperatures.
5. The value of L_ϕ in the plateau region is Chaser < Enordet < Sellogen at all temperatures. Chaser is the only surfactant of this group that exhibits an exothermic L_ϕ at higher concentrations at all temperatures.
6. Effectiveness as a foamer is associated with a sharper CMC (region 2) and a more exothermic plateau region. This suggests that Chaser is able to form aggregates at 200° C in electrolyte-free water, whereas the others are not.
7. Ethoxylated carboxylates have solution properties distinctly different from those of sulfonate surfactants.
8. A mixture of Enordet and MA-18 behaves like more dilute Enordet at 25° C, but much like the MA-18 at 125° C. This result suggests that to incorporate some of the properties of an ethoxylated surfactant to an AOS by mixing, a 1:1 mixture may well be appropriate at 25° C, but at 125°, the ratio of CES needs to be much lower than 1:1.

REFERENCES

1. Archer, D. G. Enthalpies of Dilution from 50° to 225° C of Aqueous Decyltrimethylammonium Bromide. *J. Solution Chem.*, v. 7, 1986, p. 581.
2. _____. Enthalpy of Dilution of Aqueous Sodium Chloride from 76° to 225° C and Aqueous Dodecyltrimethylammonium Bromide from 50° to 225° C. *J. Solution Chem.*, v. 15, 1986, p. 727.
3. _____. Enthalpies of Dilution of Aqueous Dodecyl- and Tetradecyl- Trimethylammonium Bromides from 323 to 448 K and of Aqueous Sodium Chloride from 349 to 448 K. Department of Energy Report No. NIPER-217, 1987. NTIS order no. DE87001221.
4. _____. Enthalpies of Dilution of Aqueous Tertradecyltrimethyl-ammonium Bromide from 50° to 175° C. *J. Solution Chem.*, v. 16, 1987, p. 347.
5. _____. Heat Capacities of Aqueous Decyl- and Dodecyl- Trimethyl-ammonium Bromides from 324.6 to 374.6 K. *J. Chem. Thermo.*, v. 19, 1987, p. 407.
6. Lam, A. C. and D. G. Archer. Enthalpies of Dilution of Dodecyl- and Tetradecyl-Trimethylammonium Bromides in Aqueous Solutions of Sodium Bromide at Elevated Temperatures. Department of Energy Report No. NIPER-304, 1987. NTIS order no. DE88001219.
7. Noll, L. A. and A. C. Lam. Effects of 1-Butanol on the Micellization of Dodecyltrimethylammonium Bromide at Elevated Temperatures. Department of Energy Report No. NIPER-368, 1988. NTIS order no. DE89000723.
8. Berg, R. L. Thermodynamics of Aqueous Sodium Dodecyl Sulfate. BERC/TPR-77/3, 1977. (Available from NIPER.)
9. De Lisi, R. and S. Milioto. Mass Action Model for Solute Distribution Between Water and Micelles. Partial Molar Volumes of Butanol and Pentanol in Dodecyl Surfactant Solutions. *J. Solution Chem.*, v. 15, 1986, p. 23.

TABLE 1. - Properties of bulk surfactants

Surfactant	% Active	Avg. molecular weight, Daltons	% Inorganic
Chaser SD1000	40	310	1
Sellogen WL	32.5	326	5
Enordet AOS 1416	39	325	3
Hüls 6.5	90.9	586	9
MA-18	90	696	-
AOS / MA-18 mixture	-	513	-

Properties of the individual surfactants were obtained from the manufacturer's literature. The properties of the mixture were calculated by averaging the properties of the individual components.

TABLE 2. - Density and apparent molar volume of Chevron Chaser SD1000 at 25° C

Concentration, % active	Density, g mL ⁻¹	V _φ , mL mol ⁻¹
0.	0.99706	-
0.0993	0.99725	251
0.2033	0.99740	259
0.2907	0.99764	249
0.3963	0.99785	249
0.7751	0.99854	252
1.5839	1.00002	253
2.4241	1.00156	253
3.1347	1.00282	254
3.8606	1.00416	254
7.7932	1.01131	255

Least-squares fit: d = 0.99710 +0.0018259·Concentration (%).

TABLE 3.- Density and apparent molar volume of Shamrock Sellogen WL at 25° C

Concentration, % active	Density, g mL ⁻¹	V_ϕ , mL mol ⁻¹
0	0.99706	—
0.06899	0.99724	241
0.1762	0.99774	201
0.2523	0.99803	201
0.3019	0.99823	200
0.7231	0.99954	215
1.2408	1.00177	203
2.0429	1.00486	203
2.6274	1.00710	203
3.2648	1.00953	203
6.6345	1.02241	205

Least squares fit: $d = 0.99701 + 0.0038286 \cdot \text{Concentration (\%)}.$

TABLE 4. - Density and apparent molar volume of Shell Enordet AOS 1416 at 25° C

Concentration, % active	Density, g mL ⁻¹	V_ϕ , mL mol ⁻¹
0.	0.99706	—
0.09568	0.99732	240
0.1853	0.99738	267
0.2646	0.99756	265
0.3553	0.99772	266
0.7717	0.99842	269
1.4758	0.99960	270
2.2035	1.00106	267
3.0353	1.00221	270
3.7906	1.00347	271
7.5563	1.00972	272
7.7103	1.00999	272

Least squares fit: $d = 0.99714 + 0.0016690 \cdot \text{Concentration (\%)}.$

TABLE 5. - Density and apparent molar volume of Hüls CES 6.5 at 25° C

Concentration, % active	Density, g mL ⁻¹	V _φ , mL mol ⁻¹
0	0.99706	-
0.2258	0.99759	450
0.4545	0.99818	443
0.6818	0.99859	456
0.9090	0.99911	456
1.8112	1.00111	457
3.6361	1.00520	456
5.4513	1.00929	457
7.2725	1.01334	458
9.0942	1.01744	458
18.1812	1.03830	459

Least squares fit: d = 0.99703 + 0.0022616·Concentration (%).

TABLE 6. - Density and apparent molar volume of Sandopan MA-18 at 25° C

Concentration, % active	Density, g mL ⁻¹	V _φ , mL mol ⁻¹
0.	0.99706	-
0.2248	0.99746	575
0.4495	0.99779	585
0.6643	0.99821	578
0.8947	0.99860	578
1.7930	0.99987	589
3.5722	1.00265	589
5.3276	1.00540	589
7.0446	1.00804	590
8.3514	1.01050	587
16.9522	1.02389	590

Least squares fit: d = 0.99708 + 0.0015810·Concentration (%).

TABLE 7. - Density and apparent molar volume of equimolar mixture of Enordet AOS 1416 and MA-18 at 25° C

Concentration, % active	Density, g mL ⁻¹	V _φ , mL mol ⁻¹
0.	0.99706	—
0.2538	0.99749	415
0.5076	0.99792	414
0.7614	0.99830	418
1.0153	0.99872	418
2.0305	1.00038	418
4.0610	1.00362	420
6.0880	1.00686	421
8.1221	1.01013	421
10.1525	1.01340	422

Least squares fit: $d = 0.99709 + 0.0016060 \cdot \text{Concentration (\%)}.$

TABLE 8. - Surface tensions at 25° C

Chaser	Sessolin		Enordet	
	% Active	Dyne/cm	% Active	Dyne/cm
4.0895	38.5	3.2551	35.0	3.9314
2.0509	39.5	1.6257	35.3	1.9658
0.4038	41.5	1.3255	35.1	0.3862
0.2022	43.0	1.0014	34.7	0.1927
0.0400	43.5	0.6682	34.0	0.0386
0.0270	45.5	0.3276	35.0	0.0243
0.0133	47.0	0.2457	37.2	0.0128
0.00399	45.5	0.1642	39.8	0.00386
0.00238	49.5	0.0826	45.0	0.00228
0.00122	52.5	0.0340	50.8	0.00123
0.000395	59.5			0.00038
				69.6

TABLE 9. - Enthalpies of dilution of Chaser SD1000 at 25° C

$P = 0.10 \text{ MPa}$ $\sigma = 0.14$				
m_i mol kg^{-1}	m_f mol kg^{-1}	ΔL_ϕ kJ mol^{-1}	Residual kJ mol^{-1}	$1/W_i$ $\% \Delta L_\phi$
0.1344	0.08112	0.173	0.093	0.7
0.1344	0.06639	0.245	0.056	1.1
0.1344	0.05138	0.366	-0.519	0.5
0.1066	0.06453	0.182	0.014	0.8
0.1066	0.05286	0.258	0.014	1.3
0.1066	0.04084	0.339	0.555	0.7
0.07932	0.04787	0.208	-0.146	1.0
0.07932	0.03947	0.287	-0.045	1.6
0.07932	0.03052	0.356	0.460	0.9
0.05245	0.03208	0.328	-1.442	0.9
0.05245	0.02618	0.332	-0.051	2.1
0.05245	0.02026	0.397	0.328	1.2
0.02602	0.01587	0.311	-0.122	1.9
0.02602	0.01302	0.443	-0.065	3.2
0.02602	0.01010	0.470	0.154	2.0
0.01296	0.007908	0.438	-0.163	2.7
0.01296	0.006500	0.511	-0.017	5.5
0.01296	0.005042	0.574	0.079	3.3
0.009707	0.005927	0.539	-0.209	3.0
0.009707	0.004866	0.541	-0.006	6.9
0.009707	0.003777	0.684	0.030	3.7
0.006465	0.003947	0.477	-0.030	5.1
0.006465	0.003239	0.607	-0.005	9.3
0.006465	0.002517	0.663	0.037	5.7
0.003229	0.001972	0.405	0.001	12
0.003229	0.001619	0.915	-0.022	12
0.003229	0.001259	0.509	0.013	15

TABLE 10. - Enthalpies of dilution of Chaser SD1000 at 125° C

$P = 1.80 \text{ MPa}$ $\sigma = 0.12$				
m_i mol kg^{-1}	m_f mol kg^{-1}	ΔL_ϕ kJ mol^{-1}	Residual kJ mol^{-1}	$1/W_i$ $\% \Delta L_\phi$
0.2726	0.1619	1.582	0.347	1.5
0.2726	0.1304	2.384	0.708	1.4
0.2726	0.1070	3.449	-0.912	0.9
0.1295	0.07801	2.282	0.045	2.1
0.1295	0.06306	3.177	0.504	2.1
0.1295	0.05192	4.591	-0.661	1.3
0.1044	0.06302	2.384	0.131	2.5
0.1044	0.05098	3.554	0.163	2.4
0.1044	0.04200	4.763	0.120	1.6
0.08014	0.04849	2.600	0.118	3.0
0.08014	0.03926	3.789	0.564	1.8
0.08014	0.03236	5.337	-0.468	1.8
0.05192	0.03150	3.098	-0.033	3.8
0.05192	0.02552	4.319	0.172	2.9
0.05192	0.02105	5.895	-0.092	2.6
0.02520	0.01533	3.355	0.060	7.2
0.02520	0.01243	5.304	-0.004	5.6
0.02520	0.01026	6.841	-0.042	4.5
0.01283	0.00782	3.975	-0.022	12
0.01283	0.00634	4.675	0.022	13
0.01283	0.00523	5.392	0.058	11
0.009404	0.00573	2.592	0.011	25
0.009404	0.00465	4.816	-0.061	9.4
0.009404	0.00384	4.900	-0.004	17
0.006571	0.00400	1.572	0.002	58
0.006571	0.00325	-0.700	0.006	70
0.006571	0.00286	3.087	-0.005	38
0.003205	0.00195	-1.840	0.000	100
0.003205	0.00159	-2.708	0.001	37
0.003205	0.00131	-3.589	0.000	67

TABLE 11. - Enthalpies of dilution of Chaser SD1000 at 200° C

P= 2.07 MPa σ = 0.326				
m_i mol kg ⁻¹	m_f mol kg ⁻¹	ΔL_ϕ kJ mol ⁻¹	Residual kJ mol ⁻¹	$1/W_i$ % ΔL_ϕ
0.1344	0.08121	4.570	-0.451	1.1
0.1344	0.06623	6.350	-0.622	1.2
0.1344	0.05585	7.460	1.671	1.2
0.1066	0.06457	4.530	-1.054	1.3
0.1066	0.05270	6.330	-0.711	2.1
0.1066	0.04446	7.250	0.435	1.5
0.07932	0.04818	4.110	0.097	2.0
0.07932	0.03935	6.140	-0.767	2.6
0.07932	0.03321	6.440	0.561	2.3
0.05245	0.03194	3.290	0.143	3.7
0.05245	0.02611	5.140	-0.759	2.8
0.05245	0.02205	4.350	0.376	5.0
0.02601	0.01588	1.050	0.003	46
0.02601	0.01299	2.460	-0.020	12
0.02601	0.01098	1.160	0.009	38
0.01296	0.007920	-0.630	0.000	150
0.01296	0.006480	0.380	0.000	150
0.01296	0.005480	0.650	0.000	140
0.009707	0.005940	-2.160	0.006	60
0.009707	0.004860	0.000	0.000	300
0.009707	0.004110	0.000	0.000	400
0.006465	0.003950	-2.380	0.002	81
0.006465	0.003230	-1.880	-0.001	61
0.006465	0.002740	-1.290	-0.001	200
0.003229	0.001980	-6.020	0.007	64
0.003229	0.001620	-5.060	0.003	59
0.003229	0.001370	-3.230	-0.001	160

TABLE 12. - Enthalpies of dilution of Sellogen WL at 25° C

P= 0.10 MPa σ = 1.8				
m_i mol kg ⁻¹	m_f mol kg ⁻¹	ΔL_ϕ kJ mol ⁻¹	Residual kJ mol ⁻¹	$1/W_i$ % ΔL_ϕ
0.1034	0.06267	0.666	2.762	0.2
0.1034	0.04999	0.940	-0.089	0.4
0.1034	0.03974	1.186	-4.191	0.2
0.08214	0.04985	0.609	-0.057	0.3
0.08214	0.03979	0.813	0.704	0.6
0.08214	0.03169	0.998	3.544	0.3
0.06119	0.03723	0.530	-0.495	0.5
0.06119	0.02971	0.733	-0.435	0.8
0.06119	0.02368	0.871	-0.397	0.5
0.04053	0.02470	0.451	-0.767	0.9
0.04053	0.01971	0.382	0.263	2.4
0.04053	0.01574	0.616	-0.064	1.0
0.02013	0.01229	0.058	0.002	13
0.02013	0.009806	-0.327	0.105	5.5
0.02013	0.007837	-0.140	-0.004	8.7
0.01003	0.006129	-0.226	-0.037	6.9
0.01003	0.004894	-0.819	0.106	4.4
0.01003	0.003913	-0.417	-0.117	5.8
0.007518	0.004593	-0.290	-0.033	7.1
0.007518	0.003668	-1.016	0.158	4.8
0.007518	0.002934	-0.604	-0.082	5.4
0.005008	0.003059	-0.370	-0.009	8.4
0.005008	0.002443	-0.896	0.045	8.1
0.005008	0.001955	-0.533	-0.026	9.1
0.002502	0.001528	-0.469	0.009	13
0.002502	0.001221	-0.039	0.000	370
0.002502	0.000977	-0.929	0.038	11

TABLE 13. - Enthalpies of dilution of Sellogen WL at 125° C

$P = 1.80 \text{ MPa}$ $\sigma = 0.22$				
m_i mol kg^{-1}	m_f mol kg^{-1}	ΔL_ϕ kJ mol^{-1}	Residual kJ mol^{-1}	$1/W_i$ $\% \Delta L_\phi$
0.2180	0.1288	3.987	-0.125	1.0
0.2180	0.08742	7.316	0.072	0.5
0.1035	0.06174	3.968	-0.061	2.2
0.1035	0.05173	4.852	0.924	0.6
0.1035	0.04207	5.783	-0.173	2.2
0.08277	0.04946	3.252	-0.042	3.3
0.08277	0.04145	4.074	-1.455	1.2
0.08277	0.03373	4.077	0.194	3.8
0.06397	0.03828	2.045	0.070	5.4
0.06397	0.03210	1.871	0.625	3.4
0.06397	0.02613	3.017	-0.062	6.7
0.03854	0.02311	1.288	0.000	140
0.03854	0.01579	0.371	-0.001	90
0.02234	0.01341	-0.307	-0.001	77
0.02234	0.009170	0.221	-0.001	150
0.009288	0.005580	-0.858	-0.001	44
0.009288	0.003820	-1.119	-0.009	37
0.007758	0.004660	-1.467	0.002	31
0.007758	0.003190	-2.396	-0.002	41
0.005413	0.003250	-3.222	0.033	20
0.005413	0.002230	-2.120	-0.004	67
0.002118	0.001270	-4.473	0.008	46
0.002118	0.000870	-3.094	-0.003	80

TABLE 14. - Enthalpies of dilution of Sellogen WL at 200° C

P= 2.07 MPa $\sigma = 0.0004$					
m_i mol kg $^{-1}$	m_f mol kg $^{-1}$	ΔL_ϕ kJ mol $^{-1}$	Residual kJ mol $^{-1}$	$1/W_i$ %	$\% \Delta L_\phi$
0.1034	0.06163	-0.394	-0.001	20	
0.1034	0.05191	-0.411	0.000	68	
0.1034	0.04214	-0.769	-0.004	15	
0.08214	0.04903	-0.754	0.014	13	
0.08214	0.04131	-0.594	0.000	59	
0.08214	0.03355	-0.737	-0.007	20	
0.06119	0.03659	-1.072	0.013	19	
0.06119	0.03084	-0.794	0.000	39	
0.06119	0.02506	-0.924	-0.005	21	
0.04053	0.02427	-1.190	0.008	25	
0.04053	0.02046	-0.918	0.000	51	
0.04053	0.01663	-0.750	-0.003	39	
0.02013	0.01208	-1.590	0.005	37	
0.02013	0.01019	-0.934	-0.001	89	
0.02013	0.008280	-1.500	-0.002	59	
0.01003	0.006020	-1.080	-0.003	74	
0.01003	0.005080	0.000	-0.004	100	
0.01003	0.004130	-5.940	0.008	30	
0.007518	0.004520	-2.550	-0.003	52	
0.007518	0.003810	0.624	0.000	350	
0.007518	0.003059	0.000	-0.001	300	
0.005008	0.003010	-0.785	-0.001	200	
0.005008	0.002540	-0.468	0.000	710	
0.005008	0.002060	-2.940	-0.001	122	
0.002502	0.001500	0.000	0.000	400	
0.002502	0.001270	1.870	0.000	350	

TABLE 15. - Enthalpies of dilution of Enordet AOS 1416 at 25° C

P= 0.10 MPa σ = 0.006				
m_i mol kg ⁻¹	m_f mol kg ⁻¹	ΔL_ϕ kJ mol ⁻¹	Residual kJ mol ⁻¹	$1/W_i$ % ΔL_ϕ
0.1255	0.07406	0.121	0.061	1.1
0.1255	0.06631	0.166	-0.049	1.5
0.1255	0.04905	0.230	-0.028	0.9
0.09909	0.05864	0.120	0.029	1.4
0.09909	0.04749	0.213	-0.110	1.8
0.09909	0.03889	0.211	0.137	1.2
0.07373	0.04375	0.124	0.008	1.8
0.07373	0.03661	0.245	-0.185	2.0
0.07373	0.02907	0.208	0.139	1.6
0.04876	0.02902	0.154	-0.021	2.1
0.04876	0.02385	0.298	-0.147	2.5
0.04876	0.01929	0.235	0.095	2.1
0.02419	0.01444	0.171	0.003	3.9
0.02419	0.01194	0.350	-0.060	4.2
0.02419	0.009572	0.134	0.034	7.4
0.01205	0.007197	0.082	0.004	16
0.01205	0.005918	0.417	-0.026	7.2
0.01205	0.004776	-0.120	0.019	16
0.009026	0.005399	0.070	0.003	25.
0.009026	0.004436	0.567	-0.043	7.0
0.009026	0.003581	-0.177	0.030	15.
0.006012	0.003597	0.141	0.005	18
0.006012	0.002728	0.723	-0.018	9
0.006012	0.002386	-0.106	0.006	37
0.003003	0.001804	0.523	-0.008	10
0.003003	0.001302	0.548	0.003	27
0.003003	0.001196	0.106	0.001	75

TABLE 16. - Enthalpies of dilution of Enordet AOS 1416 at 125° C

m_i mol kg $^{-1}$	m_f mol kg $^{-1}$	$P = 1.8 \text{ MPa}$	$\sigma = 2.29$	ΔL_ϕ kJ mol $^{-1}$	Residual kJ mol $^{-1}$	$1/W_i$ % ΔL_ϕ
0.2571	0.1532			1.460	-0.557	1.5
0.2571	0.1009			3.466	-2.560	0.6
0.2515	0.1175			1.961	1.449	1.9
0.2515	0.1175			2.183	1.041	1.7
0.1212	0.07323			2.878	1.090	1.5
0.1212	0.05765			4.440	1.689	1.7
0.1212	0.04858			6.338	1.210	0.7
0.09632	0.05835			3.621	-0.340	1.5
0.09632	0.04598			5.251	1.192	1.8
0.09632	0.03876			7.615	-2.653	0.7
0.06933	0.04212			3.686	2.441	1.6
0.06933	0.03322			7.077	0.405	1.8
0.06933	0.02802			9.940	-4.199	0.8
0.04609	0.02807			5.853	1.028	2.0
0.04609	0.02215			9.648	0.984	2.0
0.04609	0.01869			12.816	0.774	0.9
0.02393	0.01461			6.962	1.324	3.1
0.02393	0.01154			12.200	-0.381	3.0
0.02393	0.009740			14.205	-0.601	1.5
0.01097	0.006700			1.250	0.023	37
0.01097	0.005300			3.630	0.024	22
0.01097	0.004470			3.955	0.001	52
0.008163	0.004990			-3.901	0.197	16
0.008163	0.003940			2.065	-0.008	52
0.008163	0.003330			-0.477	-0.001	130
0.005713	0.003490			-4.016	0.023	22
0.005713	0.002760			-3.932	-0.012	39
0.005713	0.002330			-8.460	-0.002	11
0.002947	0.001800			-6.022	-0.024	29
0.002947	0.001200			-2.260	-0.021	78

TABLE 17. - Enthalpies of dilution of Enordet AOS 1416 at 200° C

P= 2.07 MPa σ = 0.39				
m_i mol kg ⁻¹	m_f mol kg ⁻¹	ΔL_ϕ kJ mol ⁻¹	Residual kJ mol ⁻¹	$1/W_i$ $\% \Delta L_\phi$
0.1255	0.07570	10.840	1.550	0.7
0.1255	0.06242	14.600	-1.890	0.7
0.1255	0.04742	17.730	0.550	0.6
0.09909	0.05993	9.610	0.527	2.6
0.09909	0.04946	12.250	-0.089	1.3
0.09909	0.03761	13.720	-0.322	1.0
0.07373	0.04471	6.140	0.755	2.7
0.07373	0.03692	7.700	-0.332	2.7
0.07373	0.02810	7.690	-0.007	3.5
0.04876	0.02965	1.420	0.006	17
0.04876	0.02450	1.350	0.004	19
0.04876	0.01866	1.680	0.000	240
0.02419	0.01475	-2.030	0.025	16
0.02419	0.01219	-2.820	0.020	18
0.02419	0.009290	-3.970	0.004	34
0.01205	0.007360	-3.020	0.009	22
0.01205	0.006080	-3.510	-0.002	35
0.01205	0.004640	-4.560	-0.009	35
0.009030	0.005510	-2.650	-0.003	34
0.009030	0.004560	-4.410	0.000	37
0.009030	0.003480	-3.090	-0.007	70
0.006010	0.003670	-1.660	-0.003	81
0.006010	0.003040	-6.420	0.008	39
0.006010	0.002320	-3.840	-0.005	84
0.003000	0.001520	-5.000	-0.003	49
0.003000	0.001160	-9.540	0.003	67

TABLE 18. - Enthalpies of dilution of Hüls' CES 6.5 at 25° C

P= 0.10 MPa σ = 0.0027				
m_i mol kg $^{-1}$	m_f mol kg $^{-1}$	ΔL_ϕ kJ mol $^{-1}$	Residual kJ mol $^{-1}$	$1/W_i$ $\% \Delta L_\phi$
0.3792	0.2188	-0.099	-0.011	8.1
0.3792	0.1860	-0.230	0.000	3.3
0.3792	0.1443	-0.321	0.047	0.4
0.1707	0.1020	-0.154	-0.021	3.9
0.1707	0.08736	-0.208	-0.011	5.4
0.1707	0.06842	-0.311	-0.159	0.9
0.1338	0.08012	-0.172	-0.006	4.4
0.1338	0.06905	-0.219	-0.003	8.1
0.1338	0.05413	-0.327	0.037	1.5
0.09839	0.05914	-0.195	0.007	5.2
0.09839	0.05113	-0.239	0.001	11
0.09839	0.04017	-0.338	0.103	1.5
0.06439	0.03906	-0.212	0.000	102
0.06439	0.03371	-0.257	0.001	14
0.06439	0.02652	-0.358	0.037	1.4
0.03148	0.01917	-0.347	0.041	4.9
0.03148	0.01658	-0.320	0.000	22
0.03148	0.01307	-0.386	-0.115	2.6
0.01566	0.009581	-0.509	0.052	6.6
0.01566	0.008271	-0.211	0.000	75
0.01566	0.006531	-0.619	0.009	6.5
0.01172	0.007170	-0.600	0.049	7.5
0.01172	0.006199	-0.406	0.000	47
0.01172	0.004894	-0.849	0.023	4.7
0.007791	0.004771	-0.786	0.027	8.6
0.007791	0.004119	0.040	0.000	800
0.007791	0.003254	-1.160	-0.065	5.2
0.003861	0.002367	-1.088	0.000	47
0.003861	0.002041	0.745	-0.003	86
0.003861	0.001613	-2.259	0.026	5.4

TABLE 19. - Enthalpies of dilution of Hüls' CES 6.5 at 125° C

$P = 1.80 \text{ MPa}$ $\sigma = 1.15$				
m_i mol kg^{-1}	m_f mol kg^{-1}	ΔL_ϕ kJ mol^{-1}	Residual kJ mol^{-1}	$1/W_i$ $\% \Delta L_\phi$
0.3792	0.2121	-1.053	1.630	1.0
0.3792	0.1759	-1.343	3.040	1.0
0.3792	0.1388	-0.155	-3.880	1.6
0.1707	0.09903	-0.547	0.260	4.1
0.1707	0.08280	-0.586	0.250	4.5
0.1707	0.06588	-0.545	0.070	9.1
0.1338	0.07814	-0.407	0.090	6.9
0.1338	0.06543	-0.300	0.030	11
0.1338	0.05214	-0.129	0.000	48
0.09839	0.05783	-0.085	0.000	68
0.09839	0.04850	0.201	0.000	22
0.09839	0.03870	0.577	-0.010	14
0.06439	0.03803	0.676	-0.020	13
0.06439	0.03193	0.982	-0.100	6.9
0.06439	0.02551	2.039	-0.240	6.1
0.03148	0.01873	2.621	-0.020	6.5
0.03148	0.01575	3.933	0.200	3.4
0.03148	0.01261	5.849	0.460	4.3
0.01565	0.009340	5.454	0.290	6.3
0.01565	0.007860	8.262	0.830	3.3
0.01565	0.006290	11.536	0.390	4.4
0.01172	0.007000	6.781	0.140	6.7
0.01172	0.005890	10.278	-0.460	3.5
0.01172	0.004720	12.590	-0.110	5.3
0.007791	0.004650	7.637	-0.130	9.0
0.007791	0.003920	10.849	-1.080	5.0
0.007791	0.003140	11.905	-0.300	8.5
0.003861	0.002310	3.846	-0.010	36
0.003861	0.001940	8.765	-0.350	12
0.003861	0.001560	4.360	0.000	46

TABLE 20. - Enthalpies of dilution of MA-18 at 25° C

P= 0.10 MPa σ = 0.032				
m_i mol kg ⁻¹	m_f mol kg ⁻¹	ΔL_ϕ kJ mol ⁻¹	Residual kJ mol ⁻¹	1/W _i %ΔL _φ
0.1309	0.07770	-0.311	0.000	14
0.1309	0.06580	-0.410	0.110	0.9
0.1309	0.05160	-0.562	0.227	1.2
0.1089	0.06470	-0.304	0.000	14
0.1089	0.06450	-0.236	-0.790	0.9
0.1089	0.05420	-0.404	0.078	1.2
0.1089	0.04330	-0.540	0.142	1.4
0.08090	0.04850	-0.267	-0.105	1.0
0.08090	0.04060	-0.361	-0.032	1.7
0.08090	0.03250	-0.495	0.025	2.1
0.05320	0.03210	-0.274	0.058	1.5
0.05320	0.02690	-0.318	-0.037	2.9
0.05320	0.02150	-0.453	-0.003	4.8
0.02620	0.01590	-0.205	-0.010	6.1
0.02620	0.01340	-0.291	-0.007	6.3
0.02620	0.01070	-0.348	-0.009	8.8
0.01300	0.007900	-0.236	0.004	7.0
0.01300	0.006600	-0.418	0.013	8.8
0.01300	0.005300	-0.430	-0.003	15
0.009600	0.005900	-0.260	-0.001	8.6
0.009600	0.004900	-0.534	0.013	9.3
0.009600	0.003900	-0.625	-0.002	13
0.006500	0.004000	-0.440	0.000	19
0.006500	0.003300	-0.707	0.004	10
0.006500	0.002700	-0.633	-0.012	16
0.003200	0.002000	-0.714	0.002	14
0.003200	0.001700	-1.154	0.015	13
0.003200	0.001300	-0.721	-0.008	27

TABLE 21. - Enthalpies of dilution of MA-18 at 125° C

P= 1.80 MPa σ = 0.0005				
m_i mol kg ⁻¹	m_f mol kg ⁻¹	ΔL_ϕ kJ mol ⁻¹	Residual kJ mol ⁻¹	$1/W_i$ $\% \Delta L_\phi$
0.1309	0.07568	-0.345	0.007	13
0.1309	0.06243	-0.302	0.003	17
0.1309	0.05092	-0.060	0.000	110
0.1089	0.06326	-0.320	0.009	16
0.1089	0.05224	-0.135	0.001	46
0.1089	0.04265	0.170	0.000	45
0.08085	0.04728	-0.020	0.000	370
0.08085	0.03910	0.232	0.001	36
0.08085	0.03197	0.882	-0.024	11.6
0.05323	0.03133	0.450	0.001	23
0.05323	0.02595	1.086	-0.015	11
0.05323	0.02121	1.605	-0.006	9.5
0.02623	0.01554	1.666	0.033	12
0.02623	0.01289	2.740	0.067	9.1
0.02623	0.01055	4.789	-0.024	6.3
0.01297	0.00771	3.669	0.027	11
0.01297	0.00640	5.285	0.028	12
0.01297	0.00524	7.913	-0.039	7.7
0.00961	0.00571	4.609	0.004	12
0.00961	0.00475	6.926	-0.025	13
0.00961	0.00389	8.844	-0.033	9.3
0.00649	0.00386	2.630	0.026	32
0.00649	0.00321	6.825	0.008	19
0.00649	0.00263	9.350	-0.010	13
0.00324	0.00193	3.226	0.008	52
0.00324	0.00160	3.127	0.006	83
0.00324	0.00131	7.442	0.015	33

TABLE 22. - Enthalpies of dilution of AOS / Ma-18 mixture at 25° C

P= 0.10 MPa σ = 0.0002					
m_i mol kg ⁻¹	m_f mol kg ⁻¹	ΔL_ϕ kJ mol ⁻¹	Residual kJ mol ⁻¹	1/Wi	% ΔL_ϕ
0.2204	0.1300	-0.036	0.003	4.0	
0.2204	0.1288	-0.037	0.006	3.1	
0.2204	0.1032	-0.053	0.004	4.4	
0.2204	0.09262	-0.047	-0.006	3.1	
0.2204	0.08233	-0.062	0.001	4.7	
0.1725	0.1026	-0.027	-0.002	5.1	
0.1725	0.1015	-0.032	0.000	4.6	
0.1725	0.08189	-0.043	-0.001	6.5	
0.1725	0.06734	-0.045	-0.006	5.0	
0.1725	0.06563	-0.068	0.002	5.2	
0.1265	0.07578	-0.022	-0.001	9.4	
0.1265	0.07502	-0.028	-0.001	7.7	
0.1265	0.06079	-0.033	-0.001	13	
0.1265	0.04994	-0.037	-0.003	8.5	
0.1265	0.04832	-0.079	0.004	6.5	
0.08258	0.04984	-0.024	0.000	13	
0.08258	0.04942	-0.029	0.000	11	
0.08258	0.03959	-0.009	0.000	63	
0.08258	0.03298	0.001	0.000	290	
0.08258	0.03198	-0.041	0.000	18	
0.04043	0.02460	0.046	0.000	1.0	
0.04043	0.02434	0.024	0.000	28	
0.04043	0.01965	0.065	0.001	18	
0.04043	0.01654	0.045	0.003	18	
0.04043	0.01577	0.059	0.001	26	
0.02001	0.01222	0.123	0.001	8.5	
0.02001	0.01205	0.024	0.000	51	
0.02001	0.009770	0.125	0.003	17	
0.02001	0.008220	0.060	0.003	26	
0.02001	0.007850	0.011	0.000	260	
0.01497	0.009140	0.178	-0.005	7.8	

TABLE 22. - Enthalpies of dilution of AOS / Ma-18 mixture at 25° C -- continued

$P = 0.10 \text{ MPa} \quad \sigma = 0.0002$				
m_i mol kg^{-1}	m_f mol kg^{-1}	ΔL_ϕ kJ mol^{-1}	Residual kJ mol^{-1}	$1/W_i$ $\% \Delta L_\phi$
0.01497	0.009050	-0.003	0.000	760
0.01497	0.007310	0.095	0.001	32
0.01497	0.006160	0.021	0.000	120
0.01497	0.005850	-0.136	0.003	35
0.009950	0.006080	0.330	-0.039	6.7
0.009950	0.006020	-0.060	0.001	41
0.009950	0.004900	0.054	0.000	78
0.009950	0.004100	0.053	0.000	80
0.009950	0.003920	-0.327	0.017	19
0.004960	0.003030	-0.496	-0.066	7.4
0.004960	0.003010	-0.198	0.005	25
0.004960	0.002450	-0.083	0.000	120
0.004960	0.002040	-0.267	0.007	26
0.004960	0.001940	-0.563	0.019	20

TABLE 23. - Enthalpies of dilution of AOS / MA-18 mixture at 125 °C

$P = 1.80 \text{ MPa}$ $\sigma = 0.0084$				
m_i mol kg^{-1}	m_f mol kg^{-1}	ΔL_ϕ kJ mol^{-1}	Residual kJ mol^{-1}	$1/W_i$ $\% \Delta L_\phi$
0.1928	0.1120	0.516	-0.091	9.5
0.1928	0.09088	0.946	-0.202	6.4
0.1928	0.07429	1.236	-0.132	6.0
0.1509	0.08826	0.809	-0.036	7.6
0.1509	0.07173	1.369	-0.016	6.7
0.1509	0.05871	2.215	-0.036	4.3
0.1106	0.06515	1.274	0.070	6.5
0.1106	0.05304	2.022	0.555	3.0
0.1106	0.04349	3.287	0.511	2.3
0.07223	0.04281	2.052	0.118	6.1
0.07223	0.03491	3.201	0.300	3.9
0.07223	0.02867	5.500	-0.718	2.7
0.03537	0.02109	3.861	0.045	6.5
0.03537	0.01723	6.308	-0.063	3.9
0.03537	0.01417	9.215	-0.377	4.1
0.01750	0.01047	5.232	0.219	7.7
0.01750	0.008560	8.255	0.447	4.5
0.01750	0.007040	12.189	-0.243	5.0
0.01309	0.007840	6.661	0.004	10
0.01309	0.006410	8.434	0.195	5.9
0.01309	0.005270	12.396	-0.268	6.5
0.008710	0.005220	5.187	0.034	15
0.008710	0.004270	7.955	0.003	9.4
0.008710	0.003510	8.582	0.100	10
0.004340	0.002600	5.071	-0.009	32
0.004340	0.002130	4.196	0.005	48
0.004340	0.001750	7.689	-0.021	24

TABLE 24. - Knot positions from the isothermal fits of Chaser SD1000

T/°C	25	125	200
$m^{0.5}$	10	10	10
L_ϕ	10	10	10
$m^{0.5}$	10.01	10.03	10.03
L_ϕ	-0.1	14.1	11.5
$m^{0.5}$	0.03	0.05	0.06
L_ϕ	-0.95	8.5	8.4
$m^{0.5}$	0.12	0.08	0.09
L_ϕ	-3.08	7.05	10.2
$m^{0.5}$	0.23	0.12	0.16
L_ϕ	-3.7	1.2	7.6
$m^{0.5}$	0.4	0.20	0.25
L_ϕ	-4.12	-6.0	1.5
$m^{0.5}$		0.32	0.40
L_ϕ		-11.0	-6.9
$m^{0.5}$		0.65	
L_ϕ		-15.5	

¹These knots were not allowed to vary in the least-squares minimization procedure.

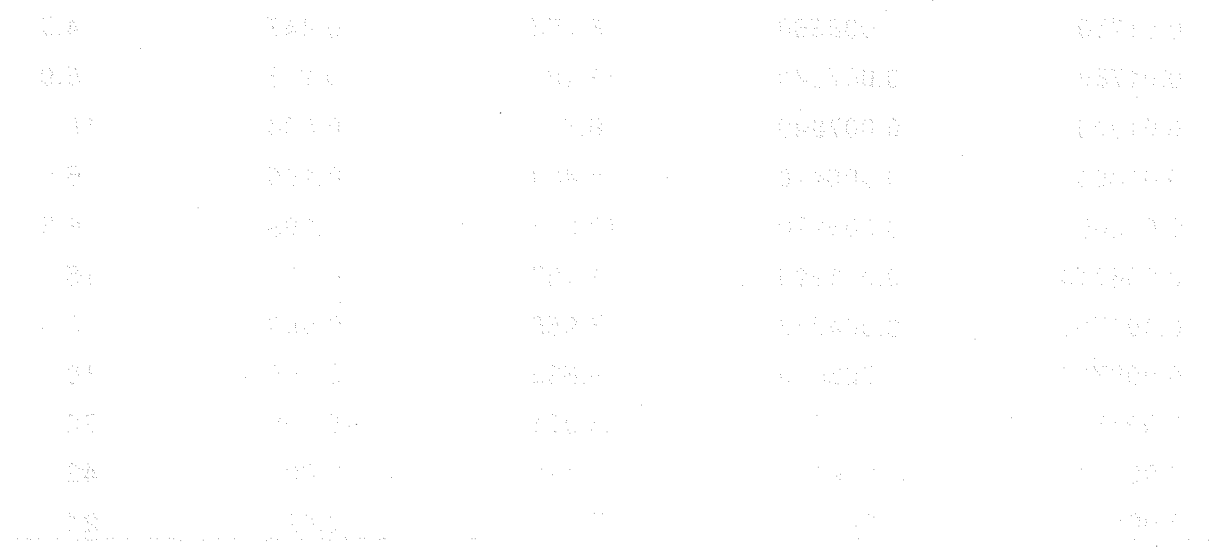


TABLE 25. - Knot positions from the isothermal fits of Sellogen WL

T/C	25	125	200
$m^{0.5}$	10	10	10
L_ϕ	10	10	10
$m^{0.5}$	10.03	0.04	0.05
L_ϕ	10.45	9.8	2.3
$m^{0.5}$	0.1	0.10	0.07
L_ϕ	2.2	16.5	6.1
$m^{0.5}$	0.15	0.15	0.09
L_ϕ	2.1	17.8	9.2
$m^{0.5}$	0.25	0.20	0.13
L_ϕ	1.2	17.3	11.3
$m^{0.5}$	0.35	0.35	0.37
L_ϕ	0.22	10.0	13.7
$m^{0.5}$		0.5	
L_ϕ		4.6	

¹These knots were not allowed to vary in the least-squares minimization procedure.

TABLE 26. - Knot positions from the isothermal fits of Enordet AOS 1416

T/°C	25	125	200
$m^{0.5}$	10	10	10
L_ϕ	10	10	10
$m^{0.5}$	0.03	0.05	0.03
L_ϕ	-1.4	34.8	12.0
$m^{0.5}$	0.10	0.10	0.10
L_ϕ	-3.2	38.4	30.2
$m^{0.5}$	0.25	0.13	0.17
L_ϕ	-3.7	30.5	33.4
$m^{0.5}$	0.40	0.18	0.23
L_ϕ	-4.0	20.1	31.0
$m^{0.5}$		0.25	0.29
L_ϕ		13.3	23.0
$m^{0.5}$		0.52	0.40
L_ϕ		6.5	8.6

¹These knots were not allowed to vary in the least-squares minimization procedure.

TABLE 27. - Knot positions from the isothermal fits of Hüls' CES 6.5

T/°C	25	125
$m^{0.5}$	10	10
L_ϕ	10	10
$m^{0.5}$	0.03	10.02
L_ϕ	4.5	10
$m^{0.5}$	0.10	10.05
L_ϕ	9.4	1-1.5
$m^{0.5}$	0.25	0.10
L_ϕ	10.3	-16.0
$m^{0.5}$	0.80	0.20
L_ϕ	11.1	-26.1
$m^{0.5}$		0.70
L_ϕ		-24.7

¹These knots were not allowed to vary in the least-squares minimization procedure.

TABLE 28. - Knot positions from the isothermal fits of Sandopan MA-18

T/°C	25	125
$m^{0.5}$	10	10
L_ϕ	10	10
$m^{0.5}$	0.03	10.02
L_ϕ	2.5	1-2.0
$m^{0.5}$	0.10	0.04
L_ϕ	5.3	-10.8
$m^{0.5}$	0.25	0.12
L_ϕ	6.2	-31.2
$m^{0.5}$	0.50	0.20
L_ϕ	7.1	-34.5
$m^{0.5}$		0.40
L_ϕ		-34.4

¹These knots were not allowed to vary in the least-squares minimization procedure.

TABLE 29. - Knot positions from the isothermal fits of AOS / MA-18 mixture

T/°C	25	125
$m^{0.5}$	10	10
L_ϕ	10	10
$m^{0.5}$	0.04	0.03
L_ϕ	-0.24	-3.8
$m^{0.5}$	0.12	0.12
L_ϕ	-0.83	-27.4
$m^{0.5}$	0.25	0.20
L_ϕ	-0.98	-36.5
$m^{0.5}$	0.52	0.52
L_ϕ	-0.89	-39.1

¹These knots were not allowed to vary in the least-squares minimization procedure.

TABLE 30. - Results of cubic spline fit: L_ϕ data for Chaser SD1000

25°C		125°C		200°C	
% Active	L_ϕ , kJ/mol	% Active	L_ϕ , kJ/mol	% Active	L_ϕ , kJ/mol
0.0000	0.000	0.0000	0.000	0.0000	0.000
0.00005	0.001	0.0003	0.059	0.0003	0.034
0.0001	0.000	0.0011	0.203	0.0011	0.058
0.0003	-0.003	0.0025	0.428	0.0025	0.085
0.0005	-0.009	0.0045	0.733	0.0045	0.129
0.0008	-0.017	0.0070	1.115	0.0070	0.203
0.0011	-0.028	0.0100	1.572	0.0100	0.320
0.0015	-0.042	0.0137	2.101	0.0137	0.495
0.0020	-0.058	0.0179	2.700	0.0179	0.741
0.0025	-0.078	0.0226	3.367	0.0226	1.072
0.0031	-0.100	0.0279	4.100	0.0279	1.500
0.0045	-0.154	0.0317	4.622	0.0337	2.034
0.0061	-0.219	0.0358	5.162	0.0402	2.659
0.0079	-0.294	0.0402	5.708	0.0471	3.352
0.0100	-0.377	0.0447	6.251	0.0547	4.094
0.0124	-0.466	0.0496	6.781	0.0627	4.862
0.0150	-0.560	0.0547	7.285	0.0714	5.635
0.0179	-0.657	0.0600	7.755	0.0806	6.393
0.0210	-0.756	0.0656	8.179	0.0903	7.114
0.0243	-0.855	0.0714	8.548	0.1006	7.777
0.0279	-0.952	0.0774	8.849	0.1115	8.360
0.0471	-1.354	0.0870	9.163	0.1229	8.848
0.0714	-1.700	0.0971	9.321	0.1349	9.244
0.1006	-1.994	0.1078	9.341	0.1474	9.557
0.1349	-2.243	0.1190	9.239	0.1604	9.797
0.1741	-2.452	0.1308	9.034	0.1741	9.973
0.2183	-2.626	0.1431	8.742	0.1882	10.09
0.2674	-2.770	0.1560	8.381	0.2030	10.17
0.3215	-2.891	0.1695	7.968	0.2183	10.20
0.3805	-2.994	0.1835	7.521	0.2341	10.21
0.4444	-3.084	0.1980	7.057	0.2505	10.20
0.5292	-3.182	0.2183	6.435	0.2908	10.14

TABLE 30. - Results of cubic spline fit: L_ϕ data for Chaser SD1000 -- continued

25°C		125°C		200°C	
% Active	L_ϕ , kJ/mol	% Active	L_ϕ , kJ/mol	% Active	L_ϕ , kJ/mol
0.6212	-3.271	0.2395	5.815	0.3342	10.02
0.7205	-3.350	0.2617	5.201	0.3805	9.850
0.8269	-3.421	0.2849	4.592	0.4298	9.640
0.9404	-3.485	0.3090	3.993	0.4820	9.389
1.061	-3.542	0.3342	3.404	0.5372	9.100
1.189	-3.593	0.3603	2.827	0.5954	8.778
1.323	-3.639	0.3874	2.265	0.6565	8.426
1.465	-3.681	0.4154	1.720	0.7205	8.047
1.613	-3.720	0.4444	1.193	0.7874	7.645
1.856	-3.776	0.5053	0.199	0.8776	7.099
2.115	-3.827	0.5701	-0.718	0.9727	6.525
2.389	-3.873	0.6387	-1.564	1.0720	5.929
2.679	-3.916	0.7111	-2.344	1.177	5.316
2.984	-3.955	0.7874	-3.064	1.286	4.690
3.304	-3.992	0.8674	-3.730	1.400	4.056
3.638	-4.026	0.9511	-4.347	1.518	3.421
3.987	-4.059	1.039	-4.920	1.641	2.787
4.350	-4.091	1.130	-5.455	1.769	2.161
		1.225	-5.958	1.901	1.548
		1.374	-6.662	2.131	0.563
		1.532	-7.309	2.373	-0.378
		1.697	-7.904	2.627	-1.281
		1.871	-8.451	2.893	-2.149
		2.053	-8.955	3.171	-2.987
		2.242	-9.419	3.460	-3.802
		2.439	-9.847	3.760	-4.596
		2.644	-10.24	4.071	-5.376
		2.857	-10.62	4.393	-6.147
		3.077	-10.96		
		3.719	-11.82		
		4.415	-12.55		
		5.161	-13.17		

TABLE 30. - Results of cubic spline fit: L_ϕ data for Chaser SD1000 -- continued

25°C		125°C		200°C	
% Active	L_ϕ , kJ/mol	% Active	L_ϕ , kJ/mol	% Active	L_ϕ , kJ/mol
100.0	0.000	100.0	-13.69	100.0	-13.69
95.0	0.000	6.796	-14.13	100.0	-13.69
90.0	0.000	7.679	-14.50	100.0	-13.69
85.0	0.000	8.602	-14.80	100.0	-13.69
80.0	0.000	9.562	-15.07	100.0	-13.69
75.0	0.000	10.56	-15.31	100.0	-13.69
70.0	0.000				
65.0	0.000				
60.0	0.000				
55.0	0.000				
50.0	0.000				
45.0	0.000				
40.0	0.000				
35.0	0.000				
30.0	0.000				
25.0	0.000				
20.0	0.000				
15.0	0.000				
10.0	0.000				
5.0	0.000				
0.0	0.000				

TABLE 31. - Results of cubic spline fit: L_ϕ data for Sellogen WL

25°C		125°C		200°C	
% Active	L_ϕ , kJ/mol	% Active	L_ϕ , kJ/mol	% Active	L_ϕ , kJ/mol
0.0000	0.000	0.0000	0.000	0.0000	0.000
0.0003	0.011	0.0005	0.191	0.0008	0.058
0.0012	0.032	0.0021	0.687	0.0033	0.100
0.0026	0.061	0.0047	1.440	0.0073	0.146
0.0047	0.098	0.0083	2.400	0.0130	0.217
0.0073	0.142	0.0130	3.518	0.0204	0.334
0.0106	0.193	0.0188	4.746	0.0293	0.519
0.0144	0.250	0.0256	6.035	0.0399	0.791
0.0188	0.312	0.0334	7.335	0.0521	1.173
0.0238	0.379	0.0422	8.599	0.0660	1.685
0.0293	0.450	0.0521	9.776	0.0814	2.348
0.0446	0.629	0.0689	11.31	0.0881	2.659
0.0631	0.820	0.0881	12.56	0.0950	2.994
0.0847	1.020	0.1095	13.58	0.1021	3.349
0.1095	1.222	0.1334	14.39	0.1095	3.719
0.1375	1.420	0.1595	15.01	0.1172	4.102
0.1687	1.609	0.1879	15.49	0.1252	4.492
0.2030	1.784	0.2187	15.85	0.1334	4.887
0.2405	1.939	0.2518	16.12	0.1418	5.281
0.2812	2.067	0.2872	16.34	0.1505	5.672
0.3249	2.165	0.3249	16.53	0.1595	6.056
0.3581	2.213	0.3581	16.69	0.1687	6.428
0.3929	2.244	0.3929	16.85	0.1782	6.789
0.4293	2.260	0.4293	17.01	0.1879	7.137
0.4672	2.262	0.4672	17.17	0.1979	7.471
0.5068	2.253	0.5068	17.31	0.2082	7.791
0.5479	2.234	0.5479	17.45	0.2187	8.096
0.5906	2.207	0.5906	17.57	0.2295	8.387
0.6349	2.174	0.6349	17.68	0.2405	8.661
0.6807	2.136	0.6807	17.77	0.2518	8.918
0.7282	2.096	0.7282	17.83	0.2634	9.158

TABLE 31. - Results of cubic spline fit: L_ϕ data for Sellogen WL -- continued

25°C		125°C		200°C	
% Active	L_ϕ , kJ/mol	% Active	L_ϕ , kJ/mol	% Active	L_ϕ , kJ/mol
0.8277	2.013	0.7771	17.87	0.2872	9.586
0.9333	1.926	0.8277	17.89	0.3121	9.949
1.045	1.838	0.8797	17.88	0.3380	10.25
1.163	1.747	0.9333	17.85	0.3650	10.51
1.287	1.654	0.9885	17.80	0.3929	10.72
1.417	1.560	1.045	17.73	0.4219	10.89
1.553	1.465	1.103	17.64	0.4519	11.03
1.695	1.369	1.163	17.54	0.4829	11.15
1.843	1.273	1.224	17.42	0.5149	11.25
1.997	1.176	1.287	17.28	0.5479	11.35
2.156	1.080	1.485	16.80	0.7672	11.85
2.321	0.984	1.695	16.21	1.0223	12.26
2.492	0.888	1.919	15.54	1.3127	12.60
2.668	0.793	2.156	14.80	1.6378	12.88
2.850	0.697	2.406	14.01	1.9968	13.09
3.038	0.602	2.668	13.19	2.389	13.27
3.230	0.507	2.943	12.35	2.814	13.40
3.428	0.411	3.230	11.52	3.270	13.51
3.632	0.316	3.529	10.72	3.756	13.60
		3.840	9.956		
		4.162	9.249		
		4.496	8.595		
		4.840	7.988		
		5.195	7.423		
		5.561	6.894		
		5.937	6.394		
		6.322	5.919		
		6.718	5.461		
		7.122	5.015		

TABLE 32. - Results of cubic spline fit: L_ϕ data for Enordet AOS 1416

25°C		125°C		200°C	
% Active	L_ϕ , kJ/mol	% Active	L_ϕ , kJ/mol	% Active	L_ϕ , kJ/mol
0.0000	0.000	0.0000	0.000	0.0000	0.000
0.0003	-0.017	0.0008	0.710	0.0003	0.232
0.0012	-0.078	0.0032	2.635	0.0012	0.807
0.0026	-0.177	0.0073	5.550	0.0026	1.676
0.0047	-0.306	0.0130	9.230	0.0047	2.793
0.0073	-0.461	0.0203	13.45	0.0073	4.108
0.0105	-0.634	0.0292	17.99	0.0105	5.574
0.0143	-0.819	0.0398	22.61	0.0143	7.142
0.0187	-1.010	0.0520	27.10	0.0187	8.764
0.0237	-1.201	0.0658	31.24	0.0237	10.39
0.0292	-1.385	0.0812	34.79	0.0292	11.98
0.0445	-1.768	0.0982	37.57	0.0445	15.35
0.0629	-2.086	0.1169	39.63	0.0629	18.27
0.0845	-2.348	0.1371	41.02	0.0845	20.78
0.1092	-2.560	0.1590	41.82	0.1092	22.92
0.1371	-2.728	0.1825	42.11	0.1371	24.73
0.1682	-2.859	0.2076	41.96	0.1682	26.24
0.2024	-2.960	0.2343	41.44	0.2024	27.51
0.2398	-3.038	0.2626	40.63	0.2398	28.56
0.2803	-3.100	0.2925	39.60	0.2803	29.44
0.3239	-3.151	0.3239	38.42	0.3239	30.20
0.4280	-3.250	0.3436	37.67	0.3707	30.85
0.5462	-3.336	0.3638	36.90	0.4206	31.43
0.6787	-3.410	0.3846	36.11	0.4736	31.91
0.8251	-3.475	0.4060	35.30	0.5297	32.33
0.9855	-3.531	0.4280	34.49	0.5888	32.67
1.160	-3.579	0.4505	33.68	0.6511	32.94
1.347	-3.620	0.4736	32.86	0.7164	33.14
1.549	-3.656	0.4972	32.05	0.7847	33.29
1.763	-3.689	0.5215	31.25	0.8561	33.38
1.991	-3.718	0.5462	30.47	0.9305	33.42

TABLE 32. - Results of cubic spline fit: L_ϕ data for Enordet AOS 1416 -- continued

25°C		125°C		200°C	
% Active	L_ϕ , kJ/mol	% Active	L_ϕ , kJ/mol	% Active	L_ϕ , kJ/mol
2.231	-3.746	0.5888	29.19	0.9967	33.41
2.485	-3.772	0.6330	27.97	1.065	33.36
2.751	-3.797	0.6787	26.79	1.136	33.28
3.029	-3.821	0.7259	25.67	1.208	33.14
3.319	-3.844	0.7748	24.60	1.283	32.95
3.621	-3.866	0.8251	23.58	1.360	32.70
3.935	-3.888	0.8771	22.62	1.440	32.39
4.260	-3.909	0.9305	21.71	1.521	32.01
4.596	-3.929	0.9855	20.86	1.605	31.56
		1.042	20.06	1.690	31.03
		1.124	19.03	1.778	30.43
		1.208	18.11	1.868	29.75
		1.296	17.28	1.960	29.02
		1.387	16.53	2.054	28.23
		1.480	15.86	2.150	27.40
		1.576	15.25	2.248	26.54
		1.676	14.70	2.348	25.66
		1.778	14.19	2.450	24.76
		1.883	13.73	2.554	23.86
		1.991	13.29	2.661	22.97
		2.433	11.78	2.860	21.38
		2.916	10.53	3.067	19.83
		3.438	9.521	3.279	18.34
		3.999	8.714	3.499	16.88
		4.596	8.082	3.724	15.45
		5.228	7.597	3.956	14.05
		5.894	7.228	4.194	12.68
		6.592	6.947	4.438	11.32
		7.321	6.724	4.687	9.976

TABLE 33. - Results of cubic spline fit: L_ϕ data for Hüls' 6.5 CES

25°C		125°C	
% Active	L_ϕ , kJ/mol	% Active	L_ϕ , kJ/mol
0.0000	0.000	0.0000	0.000
0.0005	0.080	0.0002	0.009
0.0021	0.295	0.0009	0.014
0.0047	0.623	0.0021	0.017
0.0084	1.046	0.0038	0.017
0.0132	1.544	0.0059	0.015
0.0190	2.097	0.0084	0.012
0.0258	2.686	0.0115	0.008
0.0337	3.289	0.0150	0.005
0.0427	3.889	0.0190	0.002
0.0527	4.465	0.0234	0.000
0.0802	5.649	0.0310	-0.001
0.1133	6.618	0.0396	-0.007
0.1522	7.396	0.0493	-0.030
0.1967	8.005	0.0600	-0.080
0.247	8.470	0.0717	-0.165
0.3029	8.812	0.0845	-0.298
0.3644	9.056	0.0984	-0.487
0.4315	9.225	0.1133	-0.744
0.5043	9.341	0.1293	-1.078
0.5826	9.429	0.1463	-1.500
0.7690	9.591	0.1770	-2.411
0.9806	9.730	0.2105	-3.552
1.217	9.849	0.2470	-4.882
1.478	9.950	0.2863	-6.361
1.763	10.04	0.3285	-7.947
2.072	10.11	0.3736	-9.599
2.403	10.17	0.4216	-11.28
2.758	10.22	0.4724	-12.94
3.135	10.27	0.5261	-14.54
3.533	10.31	0.5826	-16.04
5.169	10.45	0.7041	-18.66

TABLE 33. - Results of cubic spline fit: L_ϕ data for Hüls' 6.5 CES -- continued

25°C		125°C	
% Active	L_ϕ , kJ/mol	% Active	L_ϕ , kJ/mol
7.058	10.57	0.8368	-20.76
9.167	10.67	0.9806	-22.42
11.46	10.76	1.136	-23.69
13.91	10.83	1.301	-24.62
16.47	10.89	1.478	-25.27
19.11	10.94	1.665	-25.69
21.81	10.99	1.863	-25.94
24.54	11.03	2.072	-26.07
		2.29	-26.15
		3.533	-26.38
		5.01	-26.50
		6.698	-26.52
		8.572	-26.44
		10.61	-26.28
		12.78	-26.05
		15.06	-25.77
		17.42	-25.45
		19.85	-25.10

TABLE 34. - Results of cubic spline fit: L_ϕ data for MA-18

25°C		125°C	
% Active	L_ϕ , kJ/mol	% Active	L_ϕ , kJ/mol
0.0000	0.000	0.0000	0.000
0.0006	0.047	0.0003	0.004
0.0025	0.168	0.0011	-0.011
0.0056	0.351	0.0025	-0.056
0.0100	0.586	0.0045	-0.138
0.0157	0.862	0.0070	-0.270
0.0225	1.168	0.0100	-0.460
0.0307	1.494	0.0136	-0.718
0.0401	1.828	0.0178	-1.054
0.0507	2.160	0.0225	-1.478
0.0626	2.479	0.0278	-2.000
0.0952	3.136	0.0337	-2.626
0.1346	3.676	0.0401	-3.346
0.1807	4.112	0.0470	-4.145
0.2336	4.456	0.0545	-5.012
0.2932	4.721	0.0626	-5.931
0.3595	4.919	0.0712	-6.889
0.4325	5.064	0.0804	-7.872
0.5121	5.169	0.0901	-8.867
0.5984	5.246	0.1004	-9.859
0.6912	5.308	0.1112	-10.84
0.9121	5.430	0.1601	-14.46
1.163	5.542	0.2178	-17.64
1.442	5.646	0.2843	-20.41
1.751	5.742	0.3595	-22.81
2.087	5.831	0.4435	-24.87
2.451	5.915	0.5361	-26.62
2.842	5.992	0.6373	-28.10
3.259	6.066	0.7472	-29.34
3.701	6.135	0.8655	-30.38
4.169	6.202	0.9923	-31.25
5.000	6.307	1.127	-31.98

TABLE 34. - Results of cubic spline fit: L_ϕ data for MA-18 -- continued

25°C		125°C	
% Active	L_ϕ , kJ/mol	% Active	L_ϕ , kJ/mol
5.895	6.407	1.271	-32.58
6.848	6.501	1.423	-33.08
7.856	6.590	1.583	-33.47
8.915	6.676	1.751	-33.79
10.02	6.759	1.927	-34.03
11.17	6.838	2.110	-34.20
12.35	6.916	2.302	-34.34
13.57	6.993	2.502	-34.44
		2.709	-34.51
		3.259	-34.66
		3.854	-34.76
		4.494	-34.81
		5.174	-34.83
		5.895	-34.81
		6.653	-34.76
		7.447	-34.69
		8.274	-34.60
		9.132	-34.51

TABLE 35.- Results of cubic spline fit: L_ϕ data for AOS / Ma-18 mixture

25°C		125°C	
% Active	L_ϕ , kJ/mol	% Active	L_ϕ , kJ/mol
0.0000	0.000	0.0000	0.000
0.0008	0.003	0.0005	-0.035
0.0033	-0.002	0.0018	-0.165
0.0074	-0.015	0.0042	-0.382
0.0131	-0.035	0.0074	-0.680
0.0205	-0.061	0.0115	-1.051
0.0295	-0.091	0.0166	-1.488
0.0402	-0.125	0.0226	-1.984
0.0525	-0.161	0.0295	-2.531
0.0664	-0.199	0.0374	-3.123
0.0819	-0.237	0.0461	-3.752
0.1180	-0.312	0.0779	-5.812
0.1605	-0.384	0.1180	-8.086
0.2095	-0.454	0.1663	-10.52
0.2650	-0.520	0.2228	-13.06
0.3270	-0.582	0.2875	-15.65
0.3954	-0.641	0.3604	-18.23
0.4702	-0.696	0.4414	-20.76
0.5514	-0.746	0.5305	-23.17
0.6389	-0.791	0.6276	-25.42
0.7327	-0.831	0.7327	-27.45
0.8986	-0.886	0.8328	-29.03
1.081	-0.928	0.9392	-30.40
1.279	-0.958	1.052	-31.60
1.494	-0.979	1.170	-32.64
1.724	-0.992	1.295	-33.54
1.970	-0.997	1.426	-34.31
2.231	-0.998	1.563	-34.97
2.508	-0.994	1.706	-35.55
2.799	-0.988	1.855	-36.07
3.104	-0.981	2.009	-36.53
3.784	-0.966	2.685	-38.11

TABLE 35. - Results of cubic spline fit: L_ϕ data for AOS / Ma-18 mixture -- continued

25°C		125°C	
% Active	L_ϕ , kJ/mol	% Active	L_ϕ , kJ/mol
4.523	-0.954	3.449	-39.26
5.317	-0.943	4.298	-40.05
6.165	-0.933	5.227	-40.51
7.061	-0.924	6.229	-40.70
8.005	-0.916	7.302	-40.66
8.991	-0.909	8.438	-40.43
10.02	-0.902	9.632	-40.06
11.08	-0.896	10.88	-39.61

TABLE 36. - CMC's of surfactants in percent active concentration

Surfactant	25° C	125° C	200° C
Chaser SD1000	10.0032	0.11	0.23
Sellogen WL	10.32		
Sellogen WL	0.44	0.88	>4
Enordet AOS 1416	10.032	0.16	1.28
Hüls' 6.5 CES		<0.01	
Sandopan MA-18		<0.01	
AOS / MA-18 mix		<0.01	

¹These results are from surface tension measurements.

Effect of Active Concentration on Properties of Methylcellulose Polymer Chaser SD1000

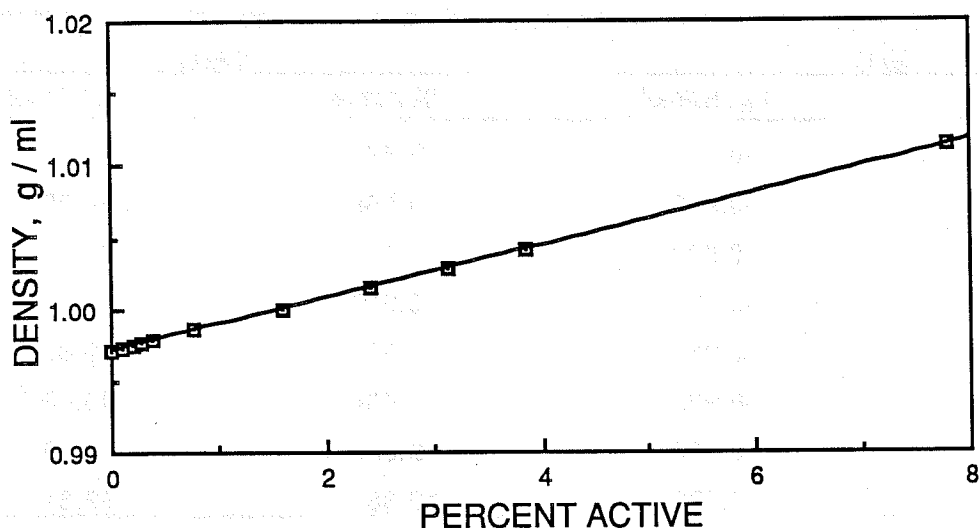


FIGURE 1. - Density of aqueous Chevron's Chaser SD1000 at 25° C.

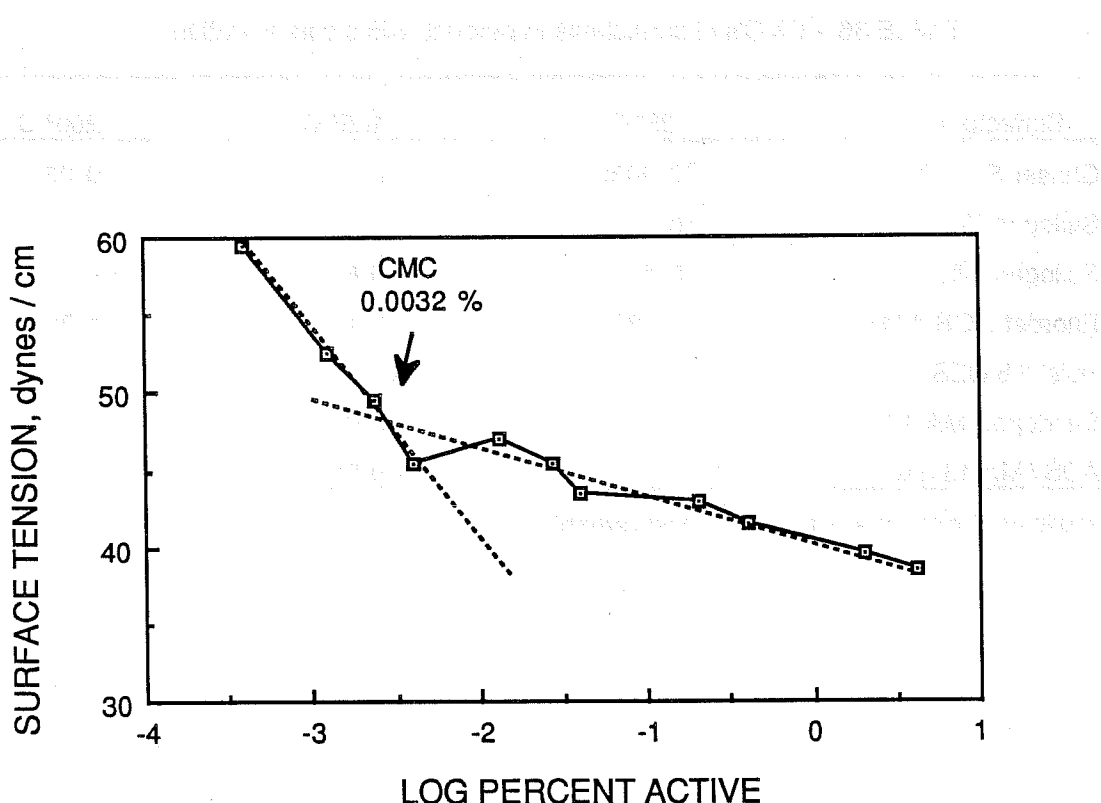


FIGURE 2. - Surface tension of Chaser SD1000 as a function of log concentration at 25° C.

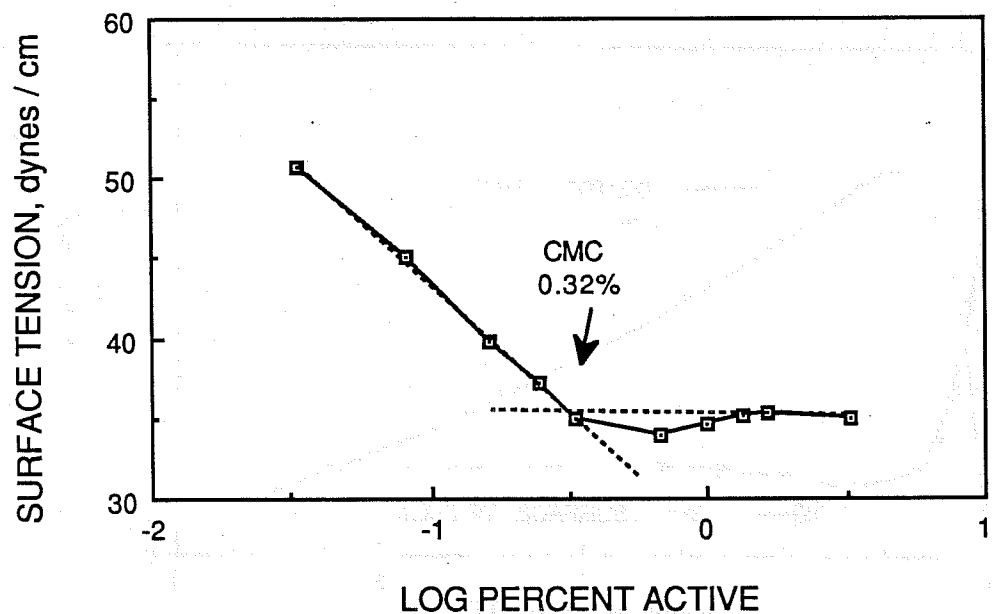


FIGURE 3. - Surface tension of Sellogen WL as a function of log concentration at 25° C.

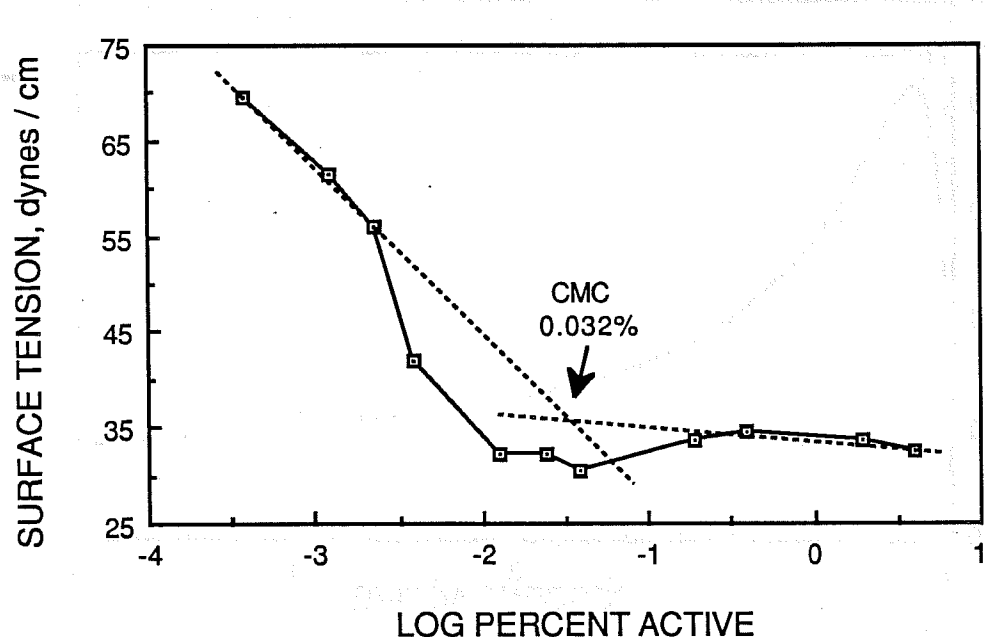


FIGURE 4. - Surface tension of Enordet AOS 1416 as a function of log concentration at 25° C.

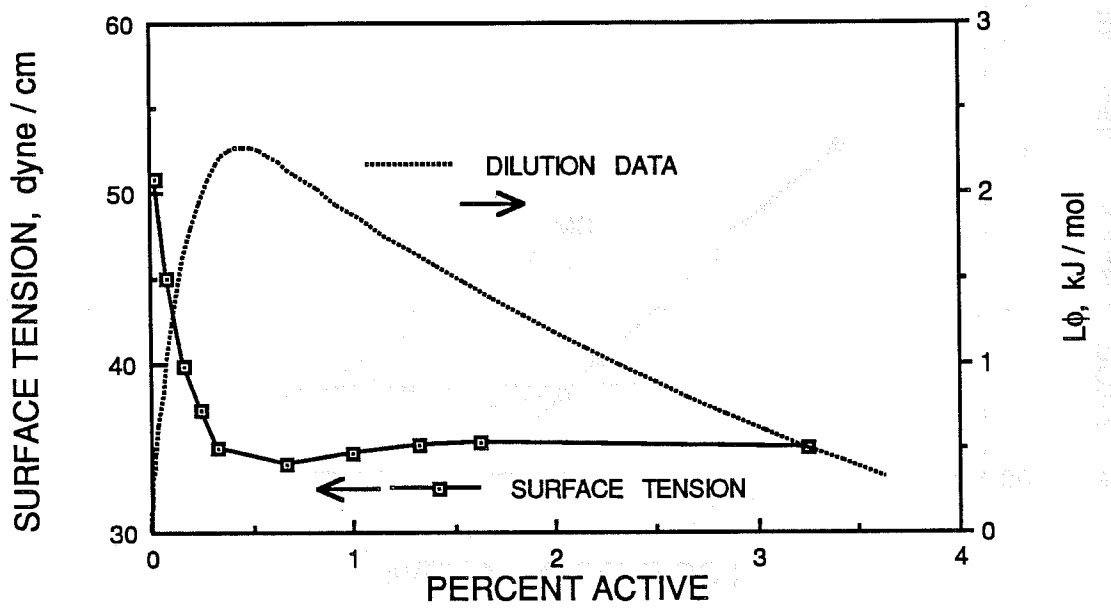


FIGURE 5. - Comparison of surface tension and relative apparent molar enthalpies of Sellogen WL at 25° C.

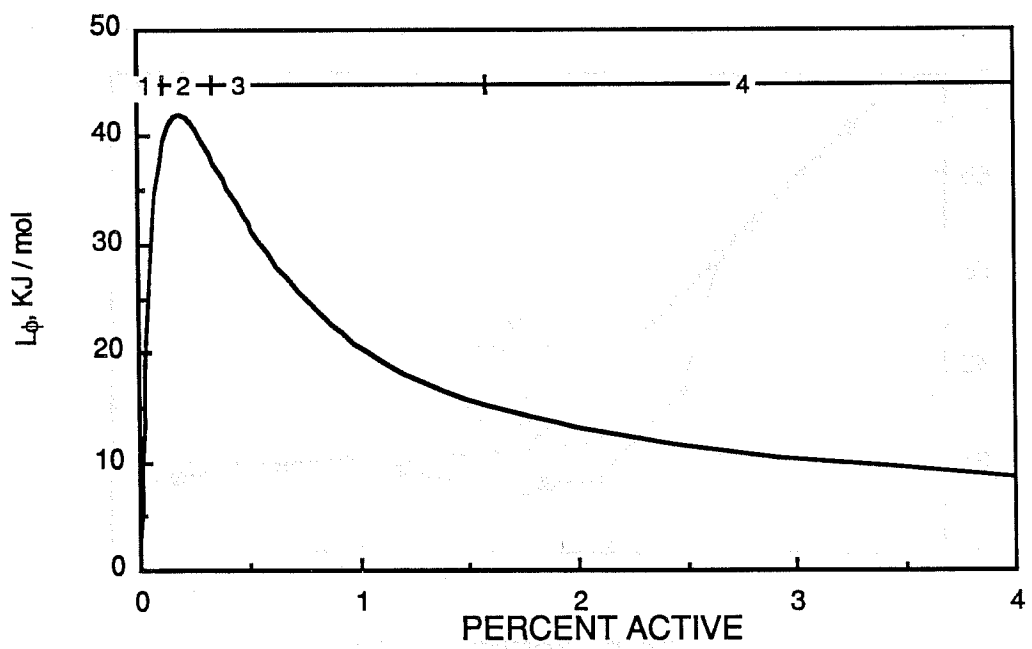


FIGURE 6. - Features of a relative apparent molar enthalpy plot. 1 is the premicellar region where monomer dilution occurs; 2 is the CMC region; 3 is the region over which aggregation phenomenon is probable; 4 is the region of dilution of micelles.

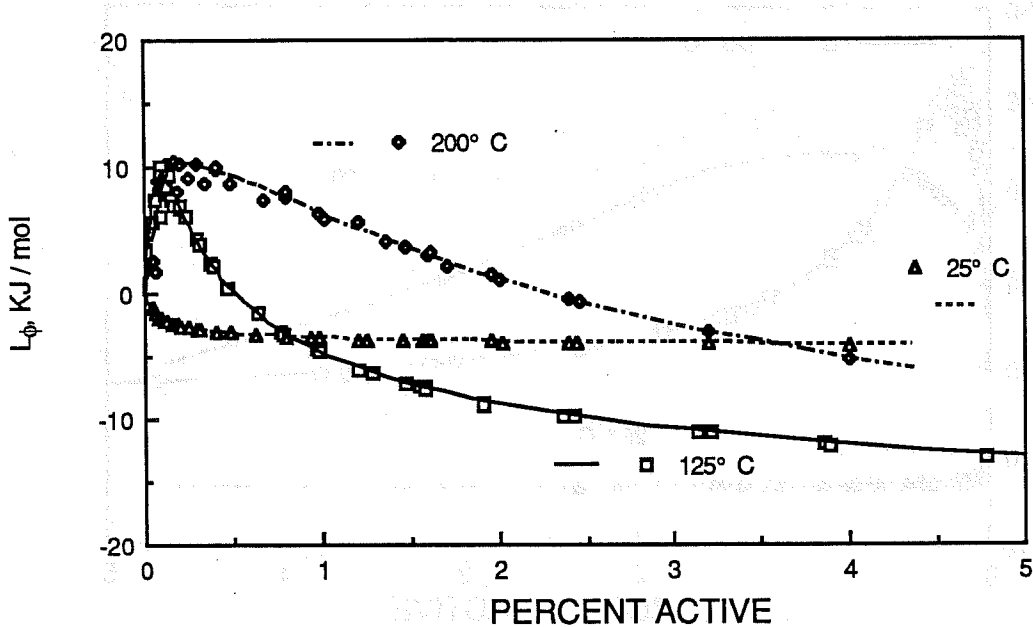


FIGURE 7. - Relative apparent molar enthalpies of Chaser SD1000 at 25°, 125°, and 200° C.

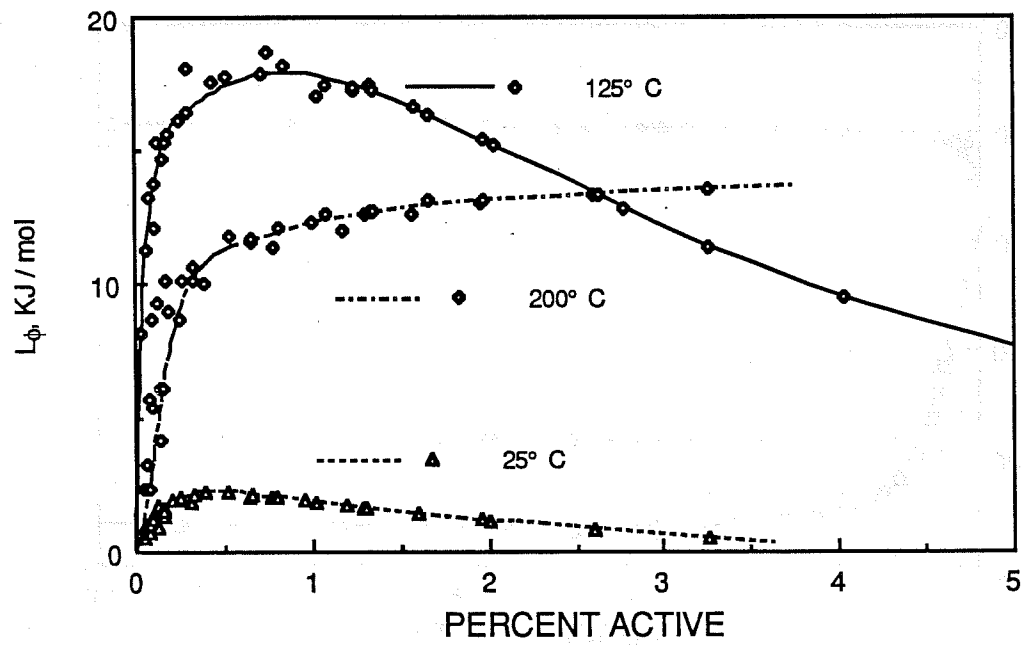


FIGURE 8. - Relative apparent molar enthalpies of Sellogen WL at 25°, 125°, and 200° C.

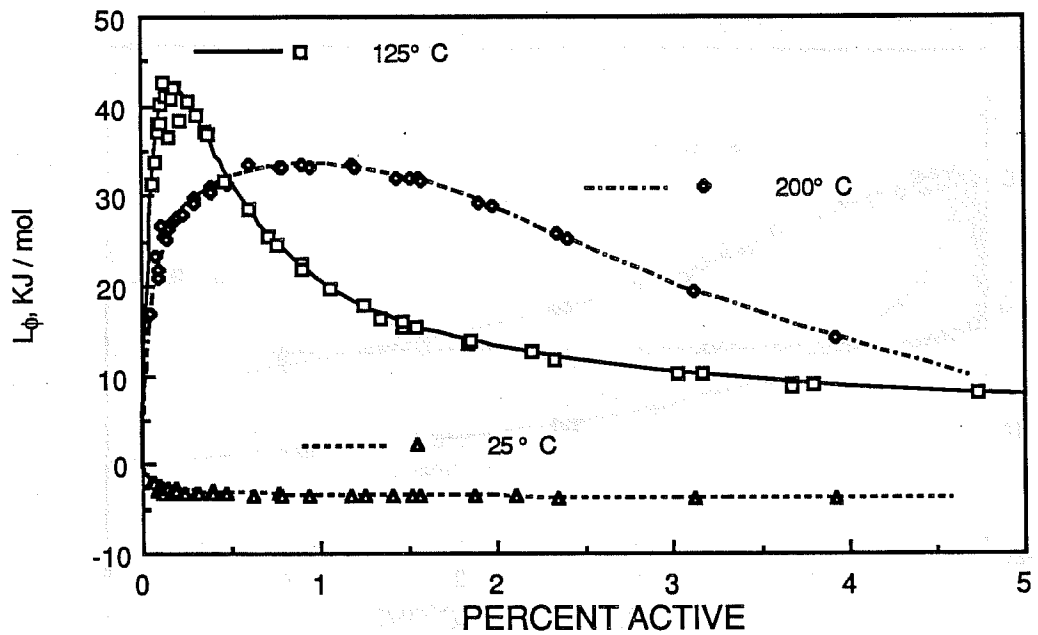


FIGURE 9. - Relative apparent molar enthalpies of Enordet AOS 1416 at 25°, 125°, and 200° C.

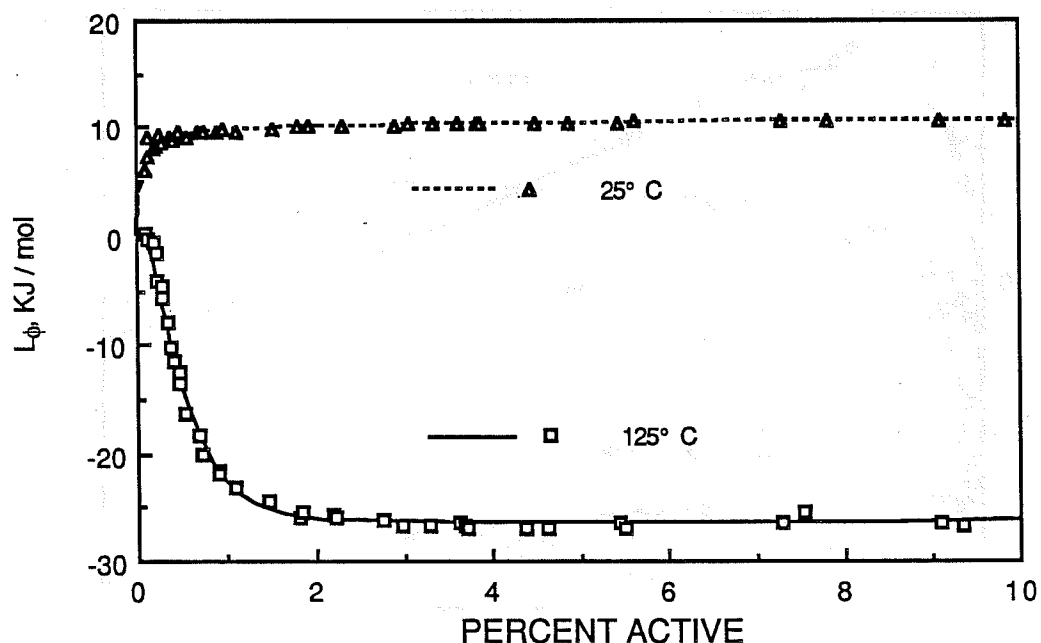


FIGURE 10. - Relative apparent molar enthalpies of Hüls' 6.5 CES at 25° and 125° C.

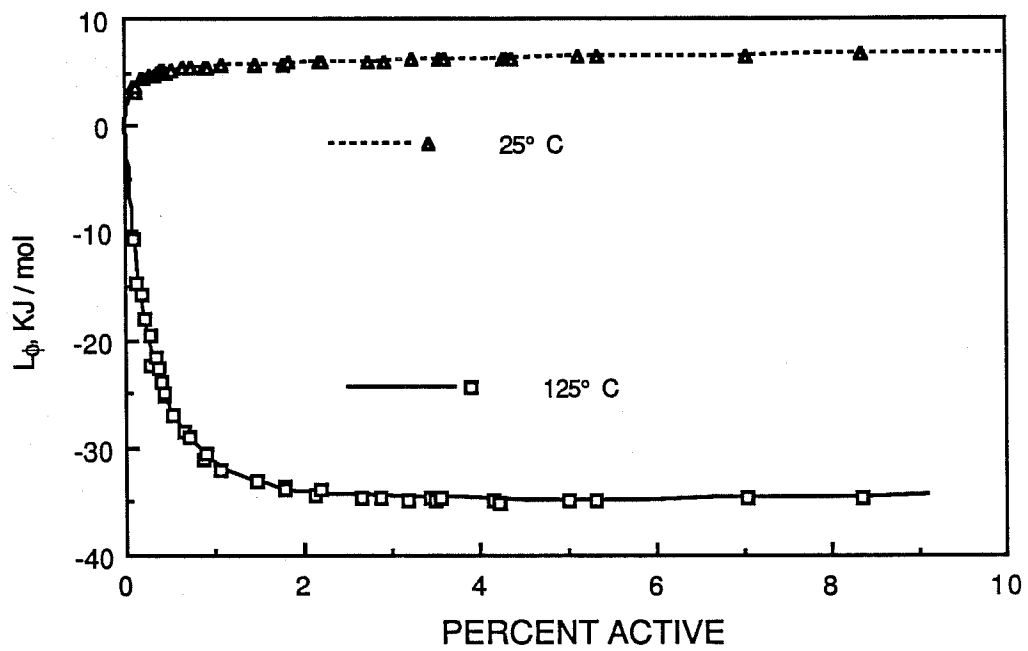


FIGURE 11 - Relative apparent molar enthalpies of Sandopan MA-18 at 25° and 125° C.

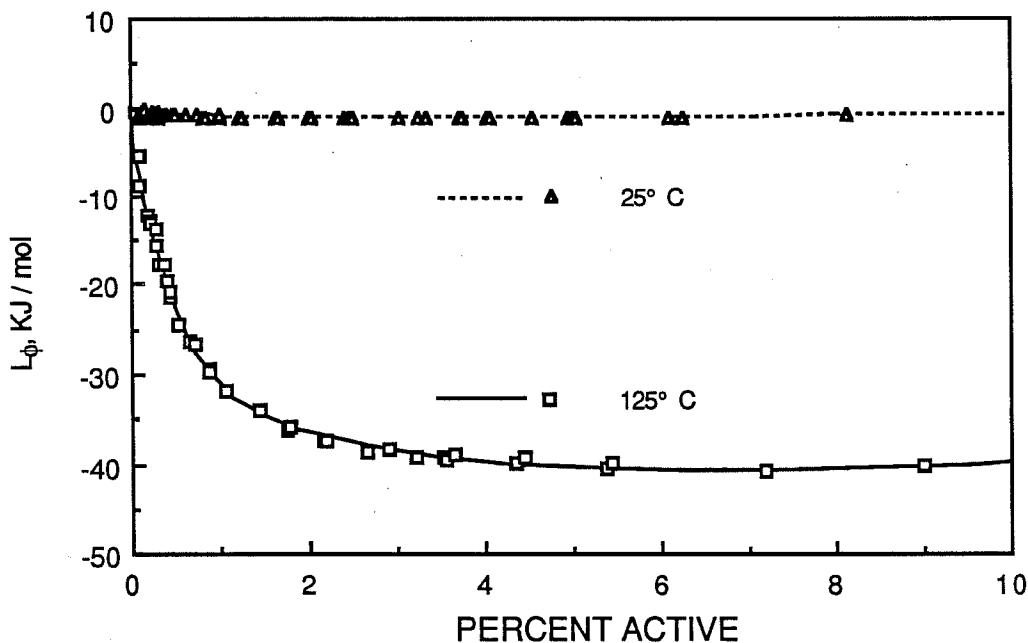


FIGURE 12. - Relative apparent molar enthalpies of AOS / MA-18 mixture at 25° and 125° C.

